AKT2 modulates astrocytic nicotine responses *in vivo.*

Andrew M. Lombardi[1], Helen Wong[2], Myra E. Bower [1,2], Ryan Milstead[1,2], Curtis Borski[2], Emily Schmitt[1], Mina Griffioen[1,2], Lauren LaPlante[2], Marissa A. Ehringer[1,2], Jerry Stitzel[1,2], and Charles A. Hoeffer[1,2,3,#]

[1]Department of Integrative Physiology, University of Colorado, Boulder, CO 80303; [2]Institute for Behavioral Genetics, University of Colorado, Boulder, CO 80309; [3]Linda Crnic Institute, Anschutz Medical Center, Aurora, CO 80045

[#]Corresponding author: Charles Hoeffer: Institute for Behavioral Genetics, University of Colorado Boulder, 1480 30th Street, Boulder, CO 80309-0447.

E-mail: charles.hoeffer@colorado.edu

Keywords: glia, nicotinic receptor, conditioned place preference, Sholl analysis

Running Title: ***AKT2 regulates astrocytic nicotine responses.***

Acknowledgments:

These studies were supported by grants from the National Institutes of Health (R01 NS086933-01, R01 AG064465, R01 AG083268, T32 MH016880, R21/R33 DA055781, and T32 AG052371) and funds from the Linda Crnic Institute. We thank Dr. Hunter Mathews, Dr. Jessica Hanson, Erin Shiely, Jaeson Chin, Sam Bingham, Andrew Cooper-Sansone, and Luke Link for their technical contributions to this work and Dr. Link's useful comments and discussions in preparing the manuscript. We acknowledge BioRender.com for the creation of the graphical abstract. We dedicate this work in the loving memory of our friend and colleague, Ms. Lauren LaPlante, whose contributions were critical to this study and the well-being of our research group.

Word Count: 7335 w/o Figure Legends, 8577 w/ Figure Legends.

Abstract

A better understanding of nicotine neurobiology is needed to reduce or prevent chronic addiction, ameliorate the detrimental effects of nicotine withdrawal, and increase successful cessation of use. Nicotine binds and activates two astrocyte-expressed nicotinic acetylcholine receptors (nAChRs), α4β2 and α7. We recently found that *Protein kinase B-β* (*Pkb-β* or *Akt2*) expression is restricted to astrocytes in mice and humans. To determine if AKT2 plays a role in astrocytic nicotinic responses, we generated astrocyte-specific *Akt2* conditional knockout (cKO) and full *Akt2* KO mice for *in vivo* and *in vitro* experiments. For *in vivo* studies, we examined mice exposed to chronic nicotine for two weeks in drinking water (200 μg/mL) and following acute nicotine challenge (0.09, 0.2 mg/kg) after 24 hrs. Our *in vitro* studies used cultured mouse astrocytes to measure nicotine-dependent astrocytic responses. We validated our approaches using lipopolysaccharide (LPS) exposure inducing astrogliosis. Sholl analysis was used to measure glial fibrillary acidic protein responses in astrocytes. Our data show that wild-type (WT) mice exhibit increased astrocyte morphological complexity during acute nicotine exposure, with decreasing complexity during chronic nicotine use, whereas *Akt2* cKO mice showed increased astrocyte morphology complexity. In culture, we found that 100μM nicotine was sufficient for morphological changes and blocking α7 or α4β2 nAChRs prevented observed morphologic changes. Finally, we performed conditioned place preference (CPP) in *Akt2* cKO mice and found that astrocytic AKT2 deficiency reduced nicotine preference compared to controls. These findings show the importance of nAChRs and *Akt2* signaling in the astrocytic response to nicotine.

Keywords: AKT2, Sholl analysis, conditional knockout, nAChR, Conditioned Place Preference, astroglia, nicotine (up to 7 allowed)

Main Points:

- Nicotine regulates astrogliosis *in vivo*: acute exposure boosts complexity; chronic exposure diminishes it.
- AKT2, expressed in astroglia, modulates morphological changes in response to nicotine and nicotine-dependent conditioned place preference.

Introduction

Astrocytes are a type of glial cell located in the central nervous system (CNS). They perform various roles, including the regulation of synaptic function (Halassa et al., 2007; Perea et al., 2009; Shigetomi et al., 2008) and homeostatic control (Ji et al., 2019; Mahmoud et al., 2019). Astrocytes release gamma-aminobutyric acid (GABA), glutamate, purines, and D-serine, maintaining extracellular ion balance (Byun et al., 2020). Compelling evidence shows that astrocytes play a role in aging and neurodegeneration (Allaman et al., 2010; Osborn et al., 2016). Alzheimer's disease (AD) patients and AD mouse models exhibit astroglial activation in a process called astrogliosis. Astrogliosis is characterized by a proinflammatory response that increases glial fibrillary acidic protein (GFAP) positive astrocytes and morphological complexity (Pekny & Nilsson, 2005; Sofroniew, 2009). In mice, astrogliosis can be induced by lipopolysaccharide (LPS), which triggers an immune reaction by activation of Toll-Like Receptors (TLR) present in astrocytes (Tarassishin et al., 2014). We can measure astrogliosis using area measurements and morphometric analysis of astrocytes called Sholl analysis (Naskar & Chattarji, 2019). Astrocytes also respond to other forms of neural stimulation such as the intake of abused substances like cocaine and opioids (Corkrum et al., 2019; Periyasamy et al., 2016), but their role in mediating neurobiological effects of drugs of abuse is not well understood.

Nicotine is one of the most widely used drugs (Jamal et al., 2016) known for being associated with the number one preventable cause of morbidity and mortality in the US, tobacco smoking. Nicotine can also impact cognition. Withdrawal from nicotine in humans is associated with deficits in memory and learning, which is also seen in mouse models of nicotine dependence (Chellian et al., 2021). Interestingly, the effects of nicotine on astrogliosis in the brain have not been described. However, nicotine may exert direct effects on astrocytes. Astrocytes express two types of nicotinic acetylcholine receptors (nAChRs) alpha7 (α7) and alpha4beta2 (α4β2) (Froeliger et al., 2015; Gahring, Persiyanov, Dunn, et al., 2004; Prado et al., 2015). These receptors are prominent in regulating astrocyte activation during inflammation and neuroprotection (Holliday & Gould, 2017; Malin et al., 1994). A protein called AKT may play a role in the astrocytic response to nicotine.

AKT (or PKB) proteins are part of a family of serine/threonine kinases with broad cellular roles. AKT signaling controls pathways essential for cell growth, proliferation, metabolism, survival, and memory processes (Cho et al., 2001; Gai et al., 2015; Levenga et al., 2021; J. Zhang et al., 2010). AKT2 is one of three AKT isoforms (AKT1/2/3) found in human and mice

brains (Cho et al., 2001; Gai et al., 2015; Levenga et al., 2017, 2021; J. Zhang et al., 2010). Our lab recently demonstrated that AKT2 was the only AKT isoform detected in mouse and human *iv vivo* astrocytes (Levenga et al., 2017, 2021). This finding is not surprising as transcriptomic analysis also shows that AKT2 is the only isoform expressed in astrocytes (Zeisel et al., 2015). Transcriptomic efforts have identified altered brain related AKT signaling in cancers (Miller et al., 2023; Tamim et al., 2014; J. Zhang et al., 2010), development (Robertson et al., 2013; D. Zhang et al., 2017), aging (Kim et al., 2022), and neurodegeneration (Allen et al., 2020; Iacobas et al., 2020). These findings suggest that AKT2 specifically regulates astrocyte function. Nicotine has been shown to activate AKT signaling (Tsurutani et al., 2005; West et al., 2003) and induce astroglial calcium responses (Araque et al., 2002; Sharma & Vijayaraghavan, 2001). Combined, these data suggest the potential for AKT2 to regulate astroglial responses to nicotine.

Our study sought to determine if nicotine exposure, both *in vivo* and *in vitro,* affected astroglial activation as measured with morpho-functional Sholl and Western analyses. We also sought to determine if AKT2, the sole AKT isoform expressed in mouse and human astrocytes *in vivo* (Levenga et al., 2017, 2021), played a role in astrocytic responses to nicotine. Our combined data obtained from hippocampal slice and cell culture preparations indicate that astrocytes respond to nicotine following both acute and chronic exposures. The data also indicate that astrocytic AKT2 activity is required for normal morphological responses to nicotine. Finally, we provide evidence that AKT2 is needed for nicotine mediated-conditioned place preference behavior, suggesting that AKT2 function is involved in the manifestation of nicotine-dependent physiological responses. This data may indicate that AKT2 may be developed for novel diagnostic and treatment avenues linked to nicotine-use disorders.

Materials and Methods

Mice

Akt2 knockout (KO*)* mice on a C57BL/6J background were used for this study (Levenga et al., 2017). To generate experimental and control groups *Akt2*$^{(+/-)}$ mice were crossed to generate *Akt2* KO and wild-type (WT) littermates for these studies. Cre-expressing mice under the neuroepithelial stem cell protein Nestin promoter (Nestin::Cre, Jax# 003771) or the *Gfap* promoter (GFAP::Cre, Jax# 024098) crossed to floxed *Akt2* mice (Jax# 026475 and Levenga et al., 2017) were used for conditional brain-specific KO of *Akt2,* Nes-*Akt2 cKO and Gfap-Akt2 cKO,* respectively. We conducted all experiments with age (4-6 months)- and sex-matched littermates. Corresponding N for either biological or technical replicates are described in each

figure. WT and *Akt2* cKO mice were divided by treatment group and genotype. Mice were kept in cages with sex-matched littermates in plastic cages on a 12:12h light:dark cycle. Lights were turned on at 0700 and the ambient temperature ranged from 22-24 °C. Food and water were given *ad lib.* Animal care and treatment procedures conformed to the University of Colorado Boulder IACUC and NIH guidelines.

Sholl Analysis

After immunostaining (Levenga et al., 2017), GFAP-positive astrocytes in the CA1 of the hippocampus at 20x magnification, were selected for Sholl analysis using Icy (ver. 2.3.0.0). 5x5 maximum projection images were used. The channel for GFAP staining was isolated and individual astrocytes were selected by zooming in and saving the resulting image. Astrocytes that had a clear nucleus, are not bunched together with other astrocytes, and have clear GFAP positive staining were selected as randomly as possible. To use selected astrocytes, images must be binarized to run the Sholl analysis plugin on ImageJ (ver. 1.53f51). In ImageJ, binarization is done using a threshold to determine foreground vs. background. Foreground pixels are colored black, and background pixels are colored white. The threshold is determined by finding the number in the threshold editing window that preserves the most contiguous astrocyte processes. This number is then used to binarize all images using batch settings. Any errant pixels that would distort Sholl analysis are colored white, resulting in their removal from analysis. Astrocyte images are then run through the Sholl analysis ImageJ plugin using the following parameters: Starting Radius: 0µm, Step Size: 10µm, and End Radius: 125µm. Batch settings are used to reduce the time it takes to run the analysis and each image is run through the plugin individually. Data is then graphed as the number of intersections versus radius. Once analyzed through the plugin, data were reported as the number of intersections vs. distance.

LPS Treatment

Mice were exposed to 5 mg/kg lipopolysaccharide (LPS, Sigma cat# L2630) or vehicle (saline, 0.9% NaCl in water) via intraperitoneal (i.p.) injections. 24 or 72 hours later, mice were sacrificed. The mice were perfused with phosphate-buffered saline (PBS) to remove blood from the brain for imaging and western blotting analysis. One brain hemisphere was post-fixed in 4% paraformaldehyde (PFA) and transferred to 30% sucrose 24-48 hours later. This hemisphere was sliced and stained for GFAP, Neuronal nuclear protein (NeuN), and Hoechst. As described earlier, GFAP+ astrocytes were used on captured images for Sholl analysis. The other hemisphere was dissected and brain regions, including the hippocampus, were saved for

western blot analysis. Brain hemispheres used for biochemistry or imaging were counterbalanced (left or right) for all procedures. The hippocampus was used for staining and western blotting.

Western Blotting

After LPS treatment and tissue extraction, slices were frozen on dry ice. Protein lysates were obtained using procedures consistent with previous studies (Levenga et al., 2017). Mouse hippocampi were homogenized via sonication and placed in lysis buffer containing: 10mM HEPES pH 7.4, 150 mM NaCl, 50mM NaF, 1mM EDTA, 1mM EGTA, and 10mM $Na_4P_2O_7$, including 1x protease inhibitor cocktail, phosphatase inhibitor cocktails II and III, and 1% of both Triton-X and Igepal. 20µg samples were made in Laemmli sample buffer and separated by size on 4-12% Bis-Tris gels. Proteins were then transferred to PDVF membranes. These blots were blocked with 0.2% I-Block dissolved in Tris-buffered saline with 0.1% Tween-20 added. Blots were incubated with primary antibodies diluted in I-Block for 24 hours at 4°C. To detect primary antibodies, blots were incubated with secondary HRP-conjugated goat anti-mouse or goat anti-rabbit (1:5000 I-Block). Signal was detected using chemiluminescence and protein levels quantified as previously described (Levenga et al., 2017). Loading controls were used for normalization of the signal.

Transcriptomics

Mice 2-6 months of age were treated with 5mg/kg of Lipopolysaccharide (LPS) or 0.9% Saline solution through intraperitoneal injection and PFC was dissected after 24 hours. Standard techniques were used for RNA isolation, sequencing and gene expression analyses. Tissue was homogenized with a glass dounce homogenizer in Trizol reagent followed by RNA extraction following manufacturer's instructions. Poly(A)-selected libraries were created using Universal Plus™ mRNA-Seq library preparation kit with NuQuant. Libraries were sequenced on Illumina NovaSeqX to produce >40M 150bp paired-end FASTQ reads. Reads were trimmed and filtered for quality using fastp (Chen et al., 2018), then aligned to the mm10 Mus Musculus genome using STAR (Dobin et al., 2013). Raw read/gene counts for alignment files were obtained using featureCounts (Liao et al., 2014), differential gene expression was analyzed using Deseq2 software (Love at al., 2014) with a significance cut-off of adjusted $P < 0.05$

Antibody Characterization

The GFAP antibody (PhosphoSolutions, #621-GFAP, used at 1:50,000), host species chicken, recognized only the expected band at 50 kDa on western blots of mouse brains. In addition, immunostaining was observed as consistent with previous reports of GFAP imaging in astrocytes (Levenga et al., 2017; Sofroniew, 2009).

The pAKT2 antibody (Cell Signaling, #8599, used at 1:750), host species rabbit, recognized only the expected band at 60 kDa on western blots of mouse brains, consistent with previous reports (Levenga et al., 2017). In addition, we verified specificity using *Akt2* knockout tissue and the 60 kDa band was not present.

The AKT2 antibody (LS Bio, # LS-C156232, used at 1:2500), host species rabbit, recognized only the expected band at 60 kDa on western blots of mouse brains, consistent with previous reports (Levenga et al., 2017). We verified the antibody by blotting *Akt2* knockout tissue, resulting in no antibody banding as expected.

The GAPDH antibody (Cell Signaling, #5174, used at 1:1000), host species rabbit, recognized only the expected band at 37 kDa on western blots of mouse brains. This is consistent with previous reports of GAPDH use in western blotting (Levenga et al., 2017, 2021; Shi et al., 2023).

The NeuN antibody (Novus, NBP1-92693, used at 1:1000), host species mouse, stained neurons exclusively. This is consistent with previous reports (Gusel'nikova & Korzhevskiy, 2015; Levenga et al., 2017).

Acute Nicotine Treatment

To test the idea that acute nicotine exposure can modulate astrogliosis, C57BL/6J (WT) mice were injected with either vehicle (saline) or nicotine (0.09 or 0.2 mg/kg). 24 hours after treatment, brains were collected for western blotting or Sholl analysis as described above.

Chronic Nicotine Treatment

To understand the effects of chronic nicotine treatment on astrocytes, mice were given either vehicle (0.2% Saccharin) or nicotine (200µg/µL in Saccharin; for taste) in their drinking water for two weeks as described in (Mathews & Stitzel, 2019). Mouse weights were collected before all experimental procedures and at the midway point. The average pre-experimental weight was 29.81 g (± 1.81 g), and the average weight at the midway point was 29.69 g (± 1.68 g). The solution was changed four times across the two-week period, and the remaining volume was measured to confirm intake. After the treatment, mice were transcardially perfused, and

mouse coronal brain slices were stained for GFAP, NeuN, and Hoechst. Astrocytes from stained slices were imaged from the CA1 using confocal microscopy for GFAP+ astrocytes, and then Sholl analysis was performed. For each slice, 10-20 astrocytes were imaged and selected pseudo-randomly from the regions of interest as described earlier. Because of the prominent role of AKT2 in cell growth (Shen et al., 2020), we tested Nes-*Akt2* cKO mice following chronic nicotine treatment.

Primary Astrocyte Culture

To generate astrocytes for experimental use, P0-P4 mouse pups were dissected to remove the brain and isolate cortical tissues. Cortical tissues were treated with 0.25% Trypsin. After digestion, cells were plated onto one T75 coated with Poly-D-Lysine. Cells were grown in Dulbecco's modified eagle medium (DMEM) supplemented with N-2 and fetal bovine serum (FBS). After one week of proliferation, the mixed cultures were shaken at 180 rpm at 37° C for 30 minutes to dissociate adherent microglia. Finally, the plates were shaken at 240 rpm at 37° C for six hours to remove adherent oligodendrocyte precursor cells. At this point, plates contained enriched astrocytes. After two weeks of growth, astrocytes were ready for experiments. This procedure was described in previous studies (Schildge et al., 2013). Astrocytes were grown on coverslips for immunostaining or on plates for making protein lysates. Once on coverslips, astrocytes were exposed to 100µM nicotine diluted in a cell culture medium, in the presence or absence of 1µM methyl lycaconitine and dihydro-beta-erythroidine, nAChR antagonists, for 24 hours.

Conditioned Place Preference

Conditioned place preference (CPP) procedures were adapted from (Kutlu et al., 2015). Briefly, the CPP chamber was set up using three connected 20 cm x 40 cm plexiglass chambers with removable dividers connecting each. Each chamber is differentiated by different wall colors and flooring materials (wire mesh of differing composition). Testing light conditions were 585 lux, with a background sound of 62.5 dB. Lighting and background sound conditions were maintained during all phases of the CPP procedure. For CPP testing, mice were placed in the CPP chamber for 15 minutes to determine baseline chamber preference for preconditioning. Starting the next day, mice in the nicotine group were given 0.35 mg/kg subcutaneously (SQ) daily and placed for 15 minutes in the CPP chamber they did not prefer on the preconditioning day. Saline injections were given to the nicotine test group in the preferred chamber. This nicotine treatment group is noted as 'Nicotine/Saline' (**Figure 6)**. Control mice (no nicotine

injections) were randomly placed in either chamber for each training day, and saline was administered regardless of preferred or non-preferred chamber. This control treatment group is described as 'Saline/Saline' (**Figure 6)**. For conditioning, mice were given injections 5 hours after their first injection and conditioned for 15 minutes a second time. Nicotine injections and conditioning occurred for 3 consecutive days. Mice in the saline groups received two saline injections 5 hours apart for 3 consecutive days. The order in which nicotine was given for the nicotine group mice was randomized each day. After 3 days of conditioning, mice were allowed full access to both chambers, and the time spent in each chamber was determined with the Ethovision XT17 video tracking system (Noldus). Entry to the chamber was only scored once the whole body, including hindlimbs, was in the zone. The starting chamber was randomized before testing. Data were shown as averaged preference scores between both testing days and the difference in time spent in the initially unpreferred chamber between the testing day and preconditioning day. No sex-dependent differences were seen; therefore, we combined both male and female data.

Statistics

Graphpad (ver 9.1.2) software was used to perform statistical analyses. All data are shown as mean ± standard error of the mean (SEM). Differences between groups were determined with either student's t-test or N-way ANOVA. Outliers were identified and removed using the ROUT method. If ANOVA showed statistical significance, it was followed by Tukey's post hoc testing. All tests were two-tailed with an alpha of $p<0.05$. For CPP, because we were asking specifically about AKT2 function and CPP performance, t-tests were calculated to determine differences between *Akt2* KO mice in the saline or nicotine conditions. WT mice were also tested as a control for CPP validity, and control WT mice CPP performance was also assessed with a t-test.

Results

Sholl and area analysis can detect morphological changes consistent with astrogliosis.

To initiate our studies, we first tested our ability to detect astroglial morphological changes in the mouse brain induced by experimental manipulation. We exposed mice to LPS (5 mg/kg) to induce astrogliosis. Using morphometric analyses, we were able to detect significantly increased size and morphological complexity of astrocytes in the hippocampus of LPS-treated

mice compared with vehicle-treated (saline) control mice (**Figure 1A-B**; Sholl analysis: $F(2,177) = 24.80$, $p < 0.0001$, area analysis: $F(2,173) = 31.35$, $p<0.0001$). Post-hoc testing for both analysis methods shows significant differences between Saline and LPS at 24 h ($p=0.0002$) and 72 h ($p<0.0001$) after treatment. Interestingly, western blot analysis of GFAP expression using hippocampal lysates obtained from these mice did not reveal any changes in GFAP levels between LPS treatments and saline (**Figure 1C**). This was not necessarily unexpected. Similar findings have been reported (Tarassishin et al., 2014; Norden et al., 2016), and we did not detect differences in GFAP protein, we did detect LPS-mediated increases in *Gfap* mRNA using transcriptomic methods (**Supplemental Figure 1**). Regardless, our morphometric analysis parameters affirm our ability to detect astrogliosis *in vivo.*

Conditional knockout (cKO) of *Akt2* in astrocytes leads to increased morphological response to LPS treatment.

Because we found in earlier studies that AKT2 protein was restricted to astrocytes (Levenga et al., 2021; Wong et al., 2020), we next sought to determine if AKT2 activity regulated astrocytic responses to LPS. We generated astrocyte-specific Akt2 cKO (GFAP-Akt2 cKO) mice to do this. AKT2 removal and astrocyte specificity were confirmed using immunohistology and western blotting of GFAP-*Akt2* cKO brain tissue (**Figure 2A**; $t=10.39$, $p<0.0001$). We then assessed whether astrocytes of GFAP-*Akt2* cKO mice respond differently than WT mice during LPS-induced astrogliosis. We found that astrocytes in *Akt2* cKO mice had the same baseline complexity as WT astrocytes (**Figure 2B-C**). At 24 h post-LPS treatment, *Akt2* cKO astrocytes showed significantly larger size and morphologic complexity when compared with WT LPS or control groups of either genotype (**Figure 2B-C**, $F(2.565, 1334) = 19.63$, post hoc testing; WT Saline vs WT LPS $p<0.01$, WT Saline vs *Akt2* KO LPS $p<0.0001$, WT LPS vs *Akt2* KO LPS $p<0.001$, WT Saline vs *Akt2* KO Saline $p<0.01$, *Akt2* KO Saline vs *Akt2* KO LPS p,0.001). Astrocytes showed similar morphological changes after area analysis. (**Figure 2D** $F(3,78) = 8.969$, $p<0.0001$, post hoc testing; $p<0.05$ WT LPS vs WT Saline, $p<0.05$ WT LPS vs *Akt2* cKO LPS, $p<0.001$ *Akt2* cKO Saline vs *Akt2* cKO LPS, $p<0.0001$ WT Saline vs *Akt2* cKO LPS) These morphological results provide evidence that AKT2 activity is required for the normal display of LPS-induced astrogliosis.

Astrocytes display dose-dependent increases in morphological complexity after acute nicotine exposure.

Having established our ability to detect astrocyte morphometric responses to LPS, we next assessed the *in vivo* effect of nicotine exposure on astrocytes. We treated WT mice with acute nicotine (0.09 or 0.2 mg/kg) via i.p. injection. At 24 hours post-nicotine exposure, we found that astrocytes became significantly larger and morphologically more complex (**Figure 3A-B;** F= 75.01, p<0.0001, p<0.0001 for all post hoc group comparisons), consistent with astrogliosis (Sofroniew, 2009). Using area analysis, we also observed significant increases in astrocyte area in the nicotine treatment groups (**Figure 3C**, F(2, 173) = 31.35), p<0.0001 with a significant dose-dependent increase in the area with both nicotine doses (**Figure 3C**, p<0.0001 for all post hoc group comparisons between Saline and LPS groups). As with our LPS treatments, we did not detect significant differences in GFAP expression between nicotine and saline-treated astrocytes using Western blot analysis (**Figure 3D)**. We performed an additional control and counted astrocytes in the imaged areas. These counts confirmed that equal numbers of astrocytes/area were present in treatment groups (**Figure 3E**) and that our Sholl measurements did not result from nicotine effects on total astrocyte numbers. Combined, these data support the idea that astrocytes *in vivo* respond morphologically to acute nicotine exposure.

Astrocytes show decreased morphological complexity following chronic nicotine exposure but show increased morphology when *Akt2* expression is conditionally removed from astrocytes.

To assess nicotinic responses in astrocytes after a longer exposure period, more aligned with human consumption, we examined the astrocytic responses following chronic nicotine exposure. To do this, we tested WT and *Akt2* cKO mice using an established model of chronic nicotine exposure (Mathews & Stitzel, 2019). Mice were given either 0.2% saccharin or nicotine (200 µg/µL in 0.2% saccharin) for two weeks in their drinking water. Average daily fluid consumption for all nicotine groups across the two-week period was 6.73 ± 0.376 mL/day. In contrast to acute exposure, we found that WT astrocytes in the hippocampus had significantly reduced morphological complexity after chronic exposure to nicotine (**Figure 4A-B;** F=19.00, p<0.0001). Because of the prominent role of AKT2 in cell growth (Shen et al., 2020), we tested Nes-*Akt2* cKO mice following chronic nicotine treatment. This enabled the brain-specific removal of *Akt2* (Levenga et al. 2017). Without nicotine exposure, cKO astrocytes were smaller than their WT counterparts (**Figure 4A-B;** F (26, 25847) = 2375, p<0.0001, p<0.0001 WT Saccharine vs cKO Saccharin). Interestingly, cKO astrocytes showed significantly increased complexity after chronic nicotine treatment, opposite of WT astrocytes (**Figure 4A-B;** F (26,

25847) = 2375, p<0.0001**,** p<0.0001 for all post hoc group comparisons. WT Nicotine vs cKO Saccharin and WT Saccharin vs cKO Nicotine not significant). When we measured the astrocyte area, consistent with Sholl's analysis, the WT astrocyte area was reduced in response to nicotine compared to the WT saccharin group (**Figure 4C**; F(3, 487) = 5.492, p=0.001, post hoc testing; WT Nicotine vs. WT Saccharine p=0.0087). Notably, WT saccharin-treated astrocytes were significantly smaller than saccharin-treated *Akt2* cKO astrocytes (post hoc testing; WT Saccharine vs. *Akt2* cKO KO Saccharine p=0.0026). However, in contrast to the Sholl data (**Figure 4B**), we did not find that *Akt2* cKO astrocytes were larger in the nicotine group compared to the *Akt2* cKO saccharin group (**Figure 4C,** post hoc testing; *Akt2* cKO Nicotine vs. *Akt2* cKO Saccharine p=0.0688). Indeed, while the trend to larger *Akt2* cKO astrocytes following chronic nicotine was evident, the effect of chronic nicotine exposure in *Akt2* cKO mice appears limited to morphological complexity and not area.

Nicotine consumption was not a factor in these findings. The average daily nicotine consumption was nearly identical between the WT and cKO groups (**Figure 4D**). Overall, the average daily consumption of nicotine was 38.46 mg/kg/day, which is consistent with previous reports where nicotine is the sole fluid source (Pietilä & Ahtee, 2000). Based on the concentration of nicotine in drinking water, the amount of nicotine consumed is consistent with or above the normal fluid intake for C57BL/6J mouse (4.82 mL daily) (Jackson Laboratory, https://phenome.jax.org/measureset/40401). Because astrocyte numbers could affect these data, astrocyte cell counts in the imaging area were performed. There were no detectable differences in total astrocyte numbers between treatment groups in the imaged Area CA1 region (**Figure 4E**). As with acute nicotine exposure, the morphometric differences we identified were not due to changes in astrocyte number in the CA1 following the drinking protocol or exposure to nicotine.

α7 nAChRs and α4β2 activity are required for responses to nicotine in cultured astrocytes.

In primary cultures of mouse astrocytes, we found that nicotine also induces astrogliosis (**Figure 5A-B;** vehicle vs 100µM Nicotine p <0.01**)**, consistent with our results in nicotine-exposed mice and in other *in vitro* studies (Aryal et al., 2021). We determined the minimum acute nicotine dose required to elicit a response in cultured astrocytes was 100 µM nicotine, detected as an increase in astrocyte area (**Figure 5A-B;** F(3,76) = 6.739, p<0.001 post hoc testing; vehicle vs 100µM Nicotine p <0.01, 1µM Nicotine vs 100µM Nicotine p<0.01, 10µM Nicotine vs 100µM Nicotine p<0.01). Next, we tested cultured astrocyte responses under

conditions of nAChR blockade. Astrocytes express α7 and α4β2 nicotinic acetylcholine receptor (nAChR) subtypes (Aryal et al., 2021). To determine if either of these nAChRs was involved in facilitating astrocytic responses to nicotine, we used antagonists for each subtype, methyl lycaconitine (MLA) for α7 nAChR and Dihydro-beta-erythroidine (DHβE) for α4β2 (Drasdo et al., 1992; Opanashuk et al., 2001). We found that astrocytes failed to significantly change morphology, as measured by area, in response to 100μM nicotine in the presence of 1 μM MLA (**Figure 5A-C;** $F(3,67)=3.774$, post hoc testing; $p = 0.0145$, vehicle vs 100μM $p < 0.05$, vehicle + MLA vs 100μM Nicotine $p < 0.05$). When 1 μM DhβE was applied to cultured astrocytes, they similarly showed a reduced response to nicotine. (**Figure 5D-F** $F(3,73) = 6.535$, $p<0.001$, post hoc testing; vehicle vs 100μM nicotine $p<0.05$, vehicle + DhβE vs 100μM Nicotine $p<0.001$**)**. We also found that *Akt2* KO astrocytes respond more severely to 100μM nicotine than WT astrocytes, replicating our earlier *in vivo* observations. (**Figure 5D-E** WT post hoc testing; vehicle vs. WT 100μM Nicotine $p < 0.05$, Akt2 KO 100μM Nicotine vs *Akt2* KO vehicle $p<0.01$, Akt2 KO 100μM Nicotine vs. WT 100μM Nicotine $p<0.01$). These data demonstrate that α7 and α4β2 nAChRs play a significant role in the astrocytic responses to nicotine.

***Akt2* cKO mice showed reduced conditioned place preference (CPP) performance compared with WT littermate controls.**

After showing that AKT2 is involved in astrocytic nicotine responses *in vivo* and *in vitro* **(Figure 2,4**), we sought to determine if astrocytic AKT2 activity regulated functional outcomes linked to nicotine exposure. Since we observed the acute effects of nicotine treatment on astrogliosis, we chose to examine the potential role of astrocytic AKT2 in the rewarding effects of nicotine. Because our experiments centered on hippocampal astrocytes, we selected the conditioned place preference (CPP) assay to examine functional outcomes related to AKT2 activity and nicotine. The CPP assay depends on hippocampal function (Ferbinteanu et al., 2001, Hitchcock et al., 2018) and is frequently employed in rodents to test the rewarding effects of stimulus on behavior, which in this case is the preference for a chamber based on its association with nicotine exposure. Following one day of preconditioning, we used a two-tiered training paradigm (**Figure 6A)** in a three-chambered CPP apparatus (**Figure 6B**) to test whether astrocyte-specific AKT2 deficiency altered CPP performance in response to a rewarding dose of nicotine**.** To validate our CPP procedures, we included a WT testing group. Confirming our ability to perform nicotine-based CPP, we found that WT mice displayed a significant preference for the chamber in which nicotine (Nicotine/Saline) was administered compared to WT controls (Saline/Saline) (**Figure 6C;** Average Both Test Days $t(18) = 2.121$, $p=0.0481$. Having confirmed

our CPP paradigm, we next assessed CPP in the context of AKT2 deficiency. To control for potential contributions of systemic AKT2 loss on CPP behavior, we used *Akt2* cKO mice (**Figure 2**) for these experiments. Using *Akt2* cKO mice we found attenuated CPP responses to nicotine (Nicotine/Saline) compared to GFAP-*Akt2* cKO controls (Saline/Saline) (**Figure 6C;** Average Both Test Days $t(17) = 1.954$, $p>0.05$. These preference differences were not due to general locomotor responses in either distance traveled (**Figure 6D;** WT distance traveled: $t(18) = 0.6619$, $p>0.05$. GFAP-*Akt2* cKO distance traveled: $t(18) = 0.4605$, $p>0.05$) or in time spent in the unpreferred chamber (exploration) between testing and preconditioning days (**Figure 6E;** WT time spent in the unpreferred chamber: $t(18) = 1.613$, $p>0.05$. GFAP-*Akt2* cKO time spent in the unpreferred chamber: $t(18) = 1.612$, $p>0.05$). Combined with our *in vivo* and *in vitro* analyses, these data show that AKT2 activity impacts functional astrocyte morphological responses to nicotine and implicates AKT2 in astrocytic function underlying fundamental cognitive processes related to the rewarding effects of nicotine during CPP. AKT2 and associated astrocytic signaling could prove useful as a drug target for nicotine use disorders by reducing the rewarding impacts of nicotine.

Discussion (2205 words)

Our study provides novel substantial evidence determining the underlying signaling in astrocyte responses to nicotine. We also provide the first evidence for an *in vivo* response to acute nicotine exposure and identify AKT2-specific function underlying the regulation of nicotine-mediated astrocytic responses. Consistent with a previous report, we show that nicotine acts through astrocytic expressed α7 nAChRs (Aryal et al., 2021). In contrast to this study, we found *in vitro* that either α7 or α4β2 receptors can mediate astrocyte responses to nicotine. Our data also link AKT2 to astrocytic functions underlying CPP behaviors related to nicotine exposure. This data indicates an essential role for astrocytes in nicotine use disorders and a critical role for AKT2 in the underlying neurobiology of nicotine use.

In a healthy central nervous system (CNS), astrocytes participate in neural/synaptic development, blood flow regulation, ion, and neurotransmitter balance, blood-brain barrier (BBB) formation, and synaptic function (Barres, 2008; Pereira & Furlan, 2010; Santello et al., 2019; Schummers et al., 2008; Simard & Nedergaard, 2004). Under normal conditions, astrocytes exist in a 'naïve' state with diverse morphology but can also be activated to undergo complex changes to their structural-functional properties in a process known as reactive astrogliosis (Pekny & Pekna, 2014; Sofroniew, 2015; Verkhratsky, Ho, et al., 2019). Reactive astrogliosis is part of the CNS's response to injury, stress, and disease (Santello et al., 2019;

Verkhratsky, Ho, et al., 2019) that can exert both protective and pathological activity depending on the type and extent of astrocyte stimulation (Pekny & Pekna, 2014; Verkhratsky, Ho, et al., 2019). Astrogliosis is characterized by a variable degree of morphological and functional changes to astrocytes (Santello et al., 2019; Verkhratsky, Ho, et al., 2019) and can be visualized and measured morphologically and biochemically. On the other hand, astrocyte asthenia (loss of morphological complexity and function) or atrophy (Verkhratsky, Ho, et al., 2019; Verkhratsky, Rodrigues, et al., 2019) is also observed in different psychiatric disorders.

Our data indicate that astrocytes respond to nicotine exposure in a time and dose-dependent fashion *in vivo*. For the first time, we show that astrocytes underwent morphological changes consistent with astrogliosis following acute exposure to nicotine *in vivo*. We also found that nicotine treatment induced these changes in a manner that scaled with increased acute nicotine dose. These *in vivo* observations parallel what we also detected using *in vitro* astrocyte culture. However, following chronic exposure *in vivo*, astrocytes reduced their overall morphological complexity, consistent with astrocytic atrophy (Verkhratsky, Rodrigues, et al., 2019). Acute and chronic nicotine exposures have well-documented differences in expression in humans, non-human primates, and rodents. Studies using resting-state functional magnetic resonance imaging (RS-fMRI) in humans demonstrate that acute nicotine exposure amplifies attention network activation. At the same time, chronic nicotine exposures reduce brain processes and synchronicity related to executive functioning and increase default mode network (DMN) function. The DMN is a large-scale brain network primarily composed of the medial prefrontal cortex, hippocampus, posterior cingulate cortex/precuneus, and angular gyrus, and increased activity in the DMN is linked to arousal and addiction affecting cognitive performance (Brooks et al., 2017; Buckner et al., 2008, Ezama et al., 2021). Altered astrocyte morphology and function are associated with liver disease and chronic pain, and astrocyte activation may adversely impact DMN function (Alshelh et al., 2018; Lin et al., 2012). Similar processes may work in people who chronically consume nicotine, where altered astrocyte morphology and signaling within brain regions associated with addiction affect network activity. In rodents, acute and chronic nicotine treatment alters 5-hydroxytryptamine (5-HT) 2A receptor (5-HT2AR) expression and electrophysiological functionality in the lateral habenula (Lhb). Acute nicotine increased the Lhb neuropil expression, while chronic nicotine treatment decreased 5-HT2AR neuropil expression to vehicle-only levels (Bombardi et al., 2020). In mice, acute nicotine increased performance efficiency following training in nose-poke operant conditioning tasks. Still, chronic nicotine exposure did not affect task performance, indicating that acute and chronic nicotine can affect cognition and neural function differently (Leach et al., 2013). It would be

interesting to repeat these experiments to determine whether astroglial function is involved in expressing these acute vs. chronic behavioral differences. Our data suggest that chronic nicotine exposure results in astroglial asthenia. Such a process would reduce the homeostatic supportive and protective functions astroglia provides to neurons and may contribute to an altered pattern of synaptic transmission associated with chronic nicotine exposure (Fujii et al., 2000; Grieder et al., 2014; Miura et al., 2006; Welsby et al., 2006).

Astrocytes express α4β2 and α7 nicotinic receptors (nAChR)s (Gahring, Persiyanov, & Rogers, 2004; Patti et al., 2007; Sharma & Vijayaraghavan, 2001), and these receptors play a prominent role in regulating astrocyte activation during inflammation and neuroprotection (Kume & Takada-Takatori, 2018; Q. Liu et al., 2018; Loram et al., 2012; Maurer et al., 2017; Pavlov et al., 2003). Several lines of study show that α4β2 nAChRs mediate many of the effects of acute nicotine on mouse behavior, including learning and memory (Davis & Gould, 2006, 2007; Kutlu et al., 2016; Marubio et al., 2003). In rodents, α7 nAChRs are involved in attention and working memory tasks (Young et al., 2004), spatial discrimination (Levin et al., 2009), immune modulation and inflammation (Kume & Takada-Takatori, 2018; Q. Liu et al., 2018; Revathikumar et al., 2016), and neuropathic pain responses (Loram et al., 2012). More recently, the direct involvement of astrocytic α7 nAChRs in associative fear memory was shown (K. Zhang et al., 2021). Our *in vitro* data suggest that α7 and α4β2 containing nAChRs can mediate normal astrocytic nicotine responses (**Figure 5**). One critical limitation of our nAChR blockade experiment is that they were performed *in vitro*. Future work to verify our *in vitro* findings will be essential to validate the nAChRs responsible for mediating nicotine effects on astrocyte populations *in vivo*. Additionally, our data does not rule out the possibility of indirect contributions from nAChRs in neuronal populations. They also do not rule out the possibility of more complex interactions between astroglial nAChRs during more long-term nicotine exposure or during development. More detailed analyses using astrocyte-specific removal or manipulation of astrocytically expressed nAChRs will be required to address the contributions of astrocyte nAChRs. This could be achieved using genetic or viral reagents, such as our conditional removal of *Akt2* from astrocytes pre- or post-developmentally. Identifying the nAChRs responsible for nicotine responsiveness may be critical in determining the signaling cascades recruited or modified during the distinct phases of nicotine exposure.

We should note that our results with chronic nicotine exposure *in vivo* differ from those reported by Aryal and colleagues (Aryal et al., 2021). There are several potential reasons for the differences in our observations. First, we delivered our nicotine via drinking water, not through

osmotic minipumps. The different approaches have advantages and disadvantages, but nicotine delivery in drinking water is well known to provide simple, chronic nicotine exposure and the induction of dependence (Matta et al., 2007). Our primary motivation to use drinking water for oral nicotine instead of minipumps was concern over the potential effects of surgery on astroglial activation in the brain. In other AKT2-related studies, we have found that AKT2 can be activated by inflammatory events such as surgery (data not shown). A second difference is that our *in vivo* analyses looked at the number of intersections over distance, whereas the previous study looked at intersections per time. Our drinking water dose (200 ug/ml for 14 days) in C57BL/6J mice generates an average blood serum concentration of ~16 ng/ml (Grabus et al., 2005). The dose used for minipump infusion in the Aryal study was set at 2 mg/kg/h for 12 days, approximating a nicotine plasma concentration of approximately 100 ng/mL (Matta et al., 2007). Therefore, it may be that our observed chronic nicotine effects differ from those of Aryal et al. because of lower overall blood serum nicotine levels in our study. Astrocytes may respond differently to a range of nicotine concentrations and exposure times. Future studies would benefit from simultaneously analyzing multiple chronic nicotine concentrations and comparing methods.

Importantly, our studies provide some mechanistic insights into the underlying regulation of astrocytic responses to nicotine. Our study is the first to report on the effects of *Akt2* deficiency on the astrocytic response to nicotine (**Figures 2, 4**). Our published research established that AKT isoforms exhibit restricted expression at the protein level in different brain cell types (Levenga et al., 2017, 2021). AKT2 is not expressed in neurons or microglia but in astrocytes of the mouse and human brains (Levenga et al., 2021). Neuroprotective effects of nAChRs are known to require AKT signaling (Kihara et al., 2001; Kume & Takada-Takatori, 2018; Shaw et al., 2002), but AKT signaling has not been studied in nicotine use. Therefore, we used conditional genetic removal of AKT2 to determine if it played a role in astrocytic responses to nicotine. Our data provide valuable information about the regulation of astrocyte morphology by nicotine. Following the acute nicotine challenge, *Akt2* cKO astrocytes displayed reduced morphological expansion compared to WT nicotine-treated astrocytes.

Conversely, chronic nicotine treatment resulted in the loss of morphological complexity in WT astrocytes but, surprisingly, generated an enhanced response in *Akt2* cKO astrocytes. These data suggest that AKT2 regulates both phases of astrocytic responses but is faciliatory for acute exposure but inhibitory following chronic nicotine experience. One strong candidate pathway that may be involved in specifying the temporal response profile to nicotine is the

translational control cascade. The AKT-mechanistic target of rapamycin (mTOR) signal cascade is essential to translational regulation, cell growth, and differentiation (Hoeffer & Klann, 2010). mTOR is activated by reactive astrogliosis (Codeluppi et al., 2009; Jeong et al., 2021) and is required for astroglial proliferation (C.-Y. Li et al., 2015). Therefore, one possibility is that AKT2 regulates the translation of nicotine-responsive astrocytic mRNAs that, in turn, control morphological and functional responses to nicotine. However, because AKT regulates numerous cellular pathways (Cho et al., 2001; Gai et al., 2015; Wong et al., 2020; J. Zhang et al., 2010), future studies using unbiased genomics and proteomics approaches will be needed to rigorously identify AKT-dependent pathways involved in manifesting morphological alterations in astrocytes following nicotine exposure.

Nicotine's potent effect on cognition, attention, and memory is believed to underlie the formation of strong drug-context associations, which can drive future nicotine use triggered by contextual or environmental cues (Davis et al., 2005; Kutlu et al., 2016). In this way, the acute effects of nicotine can promote drug-seeking behavior and escalation to chronic use driven by pathological memory formation (Markou, 2008; Markou & Paterson, 2001; Paterson & Markou, 2004). The relationship between contextual cognition and pathological memory formation was our primary motivation for examining hippocampal astrocytes (**Figure 1**). Therefore, an improved understanding of how nicotine affects cognition and memory may be critical for preventing nicotine dependence. The conditioned place preference (CPP) paradigm CPP is a classic test that assesses the rewarding properties of a drug and relies on hippocampal function (Ferbinteanu et al., 2001, Hitchcock et al., 2018). Nicotine CPP shows a typical inverted dose-response curve. Low doses are without effect, intermediate doses tend to be rewarding, and high doses either are not rewarding or can be aversive. Our experiments utilized a rewarding dose of nicotine to determine if AKT2 was involved in mediating the rewarding effects of nicotine. Our results in WT mice (**Figure 6**) are consistent with previous work on CPP (Kutlu et al., 2015; J. Liu et al., 2019). Interestingly, we saw reduced preference with conditional *Akt2* KO, consistent with recent findings that AKT isoforms play distinct roles in mouse behaviors such as spatial, contextual memory, and extinction (Wong et al., 2020). While the effect of astrocytic AKT2 deficiency was modest, these preliminary findings are the first to examine AKT2 in the acute rewarding effects of nicotine.

Given the importance of understanding molecular mechanisms underlying nicotine reward, future studies should be conducted to examine the potential role of AKT2 in other nicotine-dependent processes. Cognitive impairment is a common symptom during nicotine abstinence (Ashare et al., 2014) and another withdrawal symptom predictive of relapse

(Patterson et al., 2010; Rukstalis et al., 2005). Working memory is affected during nicotine withdrawal in humans (Hindocha et al., 2018; Nardone et al., 2020; Sweet et al., 2010) and rodents (Arthur & Levin, 2002; Levin et al., 1990, 2009). Testing if AKT2 contributes to withdrawal-induced working memory impairments is possible using working memory assays like the radial arm maze (RAM) task (Pick & Yanai, 1983; Wincott et al., 2014). Another common nicotine withdrawal symptom that has received little attention is insomnia/sleep disturbance (American Psychiatric Association & American Psychiatric Association, 2013). The lack of studies on this oft-reported withdrawal symptom is surprising because smoking cessation consistently leads to an increase in the number of nighttime arousals (D. K. Hatsukami et al., 1984, 1985; DorothyK. Hatsukami et al., 1988) and withdrawal-induced sleep disruption/insomnia during the first month of abstinence strongly predicts relapse (Boutou et al., 2008; Cummings et al., 1985; Persico, 1992; Zhou et al., 2009). Examining the role of nicotine withdrawal-induced sleep disturbances in *Akt2* cKO mice may be informative about the role of AKT2 in nicotine-withdrawal-mediated sleep fragmentation (Mathews & Stitzel, 2019). In summary, our preliminary work identifying the role of *Akt2* in other nicotine-dependent cognitive effects could be helpful and a future therapeutic target for drug abuse and addiction.

Conclusions

Besides neurons, astrocytes also affect addiction (Verkhratsky et al., 2016). We provide *in vivo* data demonstrating that astrocytes respond to nicotine exposure in a time- and dose-dependent manner. Additionally, genome-wide association studies (GWAS) have shown that genetics plays a role in addiction (Hancock et al., 2018), and our study identifying AKT2 provides an important mechanistic link between genetics and astrocyte function during nicotine dependence. AKT2 has been linked genetically to pathological astroglial activity (Tamim et al., 2014), and now, in this study, using a loss of function conditional AKT2 removal from astrocytes. Previous studies have shown that AKT is involved in the physiological mechanisms of addiction (Zhu et al., 2021) and that *Akt* plays a role in physiological responses to nicotine (Jia et al., 2016; Y. Li et al., 2019; Xu et al., 2019). Together, these data address a gap in our understanding of the role of AKT2 in nicotine use and astrocytes. While an essential first step, future studies will be needed to understand further the role of AKT2 in astrogliosis, nicotine exposure, and impacts on cognitive processes of nicotine use and withdrawal. This knowledge may allow for developing AKT2-related treatments for future therapeutic strategies to alleviate and prevent nicotine use disorders.

Figure Legends

Figure 1: Confirmation of Sholl analysis using LPS-induced inflammatory insult. WT mice were treated with LPS (i.p.) for 24 or 72 hours. (**A-B**) Sholl and area analysis was performed on hippocampal astrocytes after LPS treatment. *Above:* Unprocessed representative images of imaged hippocampal astrocytes. *Below:* Processed (Binarized) imaged astrocytes. White, GFAP; red, NeuN; blue, Hoechst. #, $p < 0.001$ for all comparisons except 24-hour LPS vs. 72-hour LPS. ANOVA, Tukey's *post hoc.* GFAP western blot staining of homogenized hippocampi. No significant differences in total GFAP expression were detected between the experimental and control groups. ANOVA, $p > .05$ for all comparisons. β-Actin and Glyceraldehyde-3-phosphate dehydrogenase (GAPDH) used for loading controls **(C)** Representative western blot images used for the generation of quantitation graph. Imaging data representative of 3 stained slices per mouse and 10 astrocytes/mouse. Biological N=3 for each group. For Westerns, N=3 for each group. Groups were alternated by sex, either 2M, 1F, or 2F, 1M.

Figure 2: Conditional removal of *Akt2* from astrocytes enhances astrogliosis response to LPS treatment. WT and *GFAP-Akt2* cKO mice were exposed to LPS, and Sholl analysis from the astrocytes in the hippocampus was performed 24 hours later**. (A)** Representative binarized images were used to analyze and quantify the LPS experiment western blot. **(B)** Sholl analysis and **(C)** area analysis was completed with significant differences found during area analysis for all groups compared to *Akt2* cKO LPS (* $P<0.05$ WT LPS vs. *Akt2* cKO LPS, # $P<0.001$ *Akt2* cKO Saline vs. *Akt2* cKO LPS, $ $P<0.0001$ WT Saline vs. *Akt2* cKO LPS) and sholl analysis for all groups compared to *Akt2* cKO LPS (* $P<0.0001$ WT LPS vs. *Akt2* cKO LPS, # $P<0.0001$ *Akt2* cKO Saline vs. *Akt2* cKO LPS, $ $P<0.0001$ WT Saline vs. *Akt2* cKO LPS). ANOVA, Tukey's post hoc testing. Imaging data representative of 3 stained slices per mouse and 10 astrocytes/mouse. Biological N=3 for each group. Groups were alternated by sex, either 2M, 1F, or 2F, 1M. For Westerns, N=9 for each genotype and 5M and 4F for each group.

Figure 3: Acute nicotine exposure promotes astrogliosis *in vivo*. Sholl analysis of hippocampal astrocytes following acute nicotine treatment (0.09 and 0.2 mg/kg) measured 24 hours after exposure compared to saline injection. **(A)** Representative of binarized astrocytes for each treatment condition. **(B)** Sholl quantification of WT responses to acute nicotine treatment. **(C)** Area analysis of WT astrocyte responses to acute nicotine treatment. **(D)** GFAP western blot of mouse hippocampal astrocytes following acute nicotine treatment. Glyceraldehyde-3-phosphate dehydrogenase (GAPDH) was used for loading controls. Quantification of Western blotting for nicotine exposure experiment. Representative images above graph. **(E)** Cell counts

for each experimental group. For Sholl analysis, p values <.001 for all group comparisons. ANOVA, Tukey's post hoc testing. Imaging data representative of 3 stained slices per mouse and 10-20 astrocytes/mouse. Biological N=3 for each group. All mice were male. For Westerns, N=12 for all WT and *Akt2* cKO treatment groups. Equal numbers of male and female mice were used for Western. No differences between sexes were detected, and data were combined into the figure panel.

Figure 4: Chronic nicotine treatment results in reduced astrocytic morphology. WT and *Akt2* cKO were exposed to nicotine chronically, and then Sholl analysis on mouse hippocampal astrocytes following nicotine treatment. **(A)** Representative binarized images from astrocytes from each experimental group. **(B)** Sholl quantification of WT and Nes-*Akt2* cKO responses to chronic nicotine treatment. (C) Area analysis of WT and Nes-*Akt2* cKO responses to chronic nicotine treatment. **(D)** Drinking consumption between nicotine WT and Nes-*Akt2* cKO groups. **(E)** Cell counts for each experimental group. $p < 0.0001$ for all group comparisons except *Akt2* cKO Saccharin vs. WT Nicotine, and *Akt2* cKO Nicotine vs. WT Saccharin, ANOVA, Tukey's post hoc testing. Imaging data representative of 3 stained slices per mouse and 10-20 astrocytes/mouse. Biological N=3 for each group. Groups were alternated by sex, either 2M, 1F, or 2F, 1M.

Figure 5: Acute nicotine treatment induces morphological changes consistent with astrogliosis in cultured astrocytes, mitigated by blocking α7 and α4β2 nicotinic acetylcholine receptors. Astrocytes from P0 mouse pups were cultured and exposed to nicotine under different conditions of nAChR blockade. Area analysis of stained astrocytes was completed on astrocytes processed using standard imaging software. **(A, D)** Representative binarized images from astrocytes from each experimental group. **(B)** Quantification of area analysis following acute nicotine treatment (vehicle, 1μM, 10μM, 100μM), **(C)** Quantification of area analysis following acute nicotine treatment (100μM) with or without and methyl lycaconitine (MLA) treatment (1μM). **(E)** Quantification of area analysis following acute nicotine treatment (*Akt2* WT vs *Akt2* cKO). *Akt2* cKO were significantly larger than WT nicotine-treated astrocytes. **(F)** Quantification of area analysis following acute nicotine treatment (100μM) Dihydro-beta-erythroidine (DHβE) treatment (1μM). For **(B)**, differences were detected between 100μM nicotine and the other treatment groups. For **(C)**, 1 μM MLA blocked responses to 100μM nicotine. For **(F)**, 1 μM DhβE blocked responses to 100μM nicotine. ##, %%, **p <0.001. #p < 0.05, #ANOVA, Tukey *post hoc.* Data from three independent cultures using 3-5 cells/coverslip.

Figure 6: *Akt2* cKO mice show impaired Conditioned Place Preference (CPP). CPP was performed on two cohorts of WT and GFAP-*Akt2* cKO mice. **(A)** The timeline for treatment and testing during the CPP experiment. Testing D1 (day 5 of the timeline), Testing D2 (day 9 of the timeline). **(B)** The CPP chamber setup is used. The two conditioning chambers are identically sized. The neutral release chamber is sized to the exact dimensions of the conditioning chamber entry portals. **(C)** Data represented as averaged preference scores (in seconds) over both testing days following CPP training. Significant differences were seen between WT Saline (Sal) and WT Nicotine (Nic), but none between *Akt2* cKO Sal and Nic. **(D)** Distance traveled during testing. No differences were detected between genotypes between Nic and Sal groups. **(E)** Time spent in the unpreferred chamber during testing. No differences were detected between either genotypes or Nic and Sal groups. *p <0.05, T-test, N=11 for WT Saline, 9 WT Nicotine, 8 *Akt2* cKO Saline, 12 *Akt2* cKO Nicotine. Data was collected from three independent behavioral cohorts for each genotype. WT Groups: Saline 6M, 5F; Nicotine 5M, 4F. *Akt2* KO Groups: split evenly between male and female mice.

References

Allaman, I., Gavillet, M., Belanger, M., Laroche, T., Viertl, D., Lashuel, H. A., & Magistretti, P. J. (2010). Amyloid- Aggregates Cause Alterations of Astrocytic Metabolic Phenotype: Impact on Neuronal Viability. *Journal of Neuroscience*, *30*(9), 3326–3338. https://doi.org/10.1523/JNEUROSCI.5098-09.2010

Allen, S. P., Seehra, R. S., Heath, P. R., Hall, B. P. C., Bates, J., Garwood, C. J., Matuszyk, M. M., Wharton, S. B., & Simpson, J. E. (2020). Transcriptomic Analysis of Human Astrocytes In Vitro Reveals Hypoxia-Induced Mitochondrial Dysfunction, Modulation of Metabolism, and Dysregulation of the Immune Response. *International Journal of Molecular Sciences*, *21*(21), 8028. https://doi.org/10.3390/ijms21218028

Alshelh, Z., Marciszewski, K. K., Akhter, R., Di Pietro, F., Mills, E. P., Vickers, E. R., Peck, C. C., Murray, G. M., & Henderson, L. A. (2018). Disruption of default mode network

dynamics in acute and chronic pain states. *NeuroImage: Clinical*, *17*, 222–231. https://doi.org/10.1016/j.nicl.2017.10.019

American Psychiatric Association, & American Psychiatric Association (Eds.). (2013). *Diagnostic and statistical manual of mental disorders: DSM-5* (5th ed). American Psychiatric Association.

Araque, A., Martín, E. D., Perea, G., Arellano, J. I., & Buño, W. (2002). Synaptically released acetylcholine evokes Ca2+ elevations in astrocytes in hippocampal slices. *The Journal of Neuroscience: The Official Journal of the Society for Neuroscience*, *22*(7), 2443–2450. https://doi.org/10.1523/JNEUROSCI.22-07-02443.2002

Arthur, D., & Levin, E. (2002). Chronic inhibition of α4β2 nicotinic receptors in the ventral hippocampus of rats: Impacts on memory and nicotine response. *Psychopharmacology*, *160*(2), 140–145. https://doi.org/10.1007/s00213-001-0961-6

Aryal, S. P., Fu, X., Sandin, J. N., Neupane, K. R., Lakes, J. E., Grady, M. E., & Richards, C. I. (2021). Nicotine induces Morphological and Functional Changes in Astrocytes via nicotinic receptor activity. *Glia*, *69*(8), 2037. https://doi.org/10.1002/glia.24011

Ashare, R. L., Falcone, M., & Lerman, C. (2014). Cognitive function during nicotine withdrawal: Implications for nicotine dependence treatment. *Neuropharmacology*, *76*, 581–591. https://doi.org/10.1016/j.neuropharm.2013.04.034

Barres, B. A. (2008). The mystery and magic of glia: A perspective on their roles in health and disease. *Neuron*, *60*(3), 430–440. https://doi.org/10.1016/j.neuron.2008.10.013

Bombardi, C., Delicata, F., Tagliavia, C., Pierucci, M., Deidda, G., Casarrubea, M., De Deurwaerdère, P., & Di Giovanni, G. (2020). Acute and Chronic Nicotine Exposures Differentially Affect Central Serotonin 2A Receptor Function: Focus on the Lateral Habenula. *International Journal of Molecular Sciences*, *21*(5), 1873. https://doi.org/10.3390/ijms21051873

Boutou, A. K., Tsiata, E. A., Pataka, A., Kontou, P. K., Pitsiou, G. G., & Argyropoulou, P. (2008). Smoking cessation in clinical practice: Predictors of six-month continuous abstinence in a sample of Greek smokers. *Primary Care Respiratory Journal*, *17*(1), 32–38. https://doi.org/10.3132/pcrj.2008.00009

Brooks, S. J., Ipser, J., & Stein, D. J. (2017). Chronic and Acute Nicotine Exposure Versus Placebo in Smokers and Nonsmokers. In *Addictive Substances and Neurological Disease* (pp. 319–338). Elsevier. https://doi.org/10.1016/B978-0-12-805373-7.00028-1

Buckner, R. L., Andrews-Hanna, J. R., & Schacter, D. L. (2008). *The Brain's Default Network*: *Anatomy, Function, and Relevance to Disease*. *Annals of the New York Academy of Sciences*, *1124*(1), 1–38. https://doi.org/10.1196/annals.1440.011

Byun, J. S., Lee, C. O., Oh, M., Cha, D., Kim, W.-K., Oh, K.-J., Bae, K.-H., Lee, S.-C., & Han, B.-S. (2020). Rapid differentiation of astrocytes from human embryonic stem cells. *Neuroscience Letters*, *716*, 134681. https://doi.org/10.1016/j.neulet.2019.134681

Chellian, R., Behnood-Rod, A., Bruijnzeel, D. M., Wilson, R., Pandy, V., & Bruijnzeel, A. W. (2021). Rodent models for nicotine withdrawal. *Journal of Psychopharmacology (Oxford, England)*, *35*(10), 1169–1187. https://doi.org/10.1177/02698811211005629

Shifu Chen, Yanqing Zhou, Yaru Chen, Jia Gu, fastp: an ultra-fast all-in-one FASTQ preprocessor, *Bioinformatics*, Volume 34, Issue 17, September 2018, Pages i884–i890, https://doi.org/10.1093/bioinformatics/bty560

Cho, H., Mu, J., Kim, J. K., Thorvaldsen, J. L., Chu, Q., Crenshaw, E. B., Kaestner, K. H., Bartolomei, M. S., Shulman, G. I., & Birnbaum, M. J. (2001). Insulin Resistance and a Diabetes Mellitus-Like Syndrome in Mice Lacking the Protein Kinase Akt2 (PKBβ). *Science*, *292*(5522), 1728–1731. https://doi.org/10.1126/science.292.5522.1728

Codeluppi, S., Svensson, C. I., Hefferan, M. P., Valencia, F., Silldorff, M. D., Oshiro, M., Marsala, M., & Pasquale, E. B. (2009). The Rheb–mTOR Pathway Is Upregulated in

Reactive Astrocytes of the Injured Spinal Cord. *The Journal of Neuroscience*, *29*(4), 1093–1104. https://doi.org/10.1523/JNEUROSCI.4103-08.2009

Corkrum, M., Rothwell, P. E., Thomas, M. J., Kofuji, P., & Araque, A. (2019). Opioid-Mediated Astrocyte-Neuron Signaling in the Nucleus Accumbens. *Cells*, *8*(6), E586. https://doi.org/10.3390/cells8060586

Cummings, K. M., Giovino, G., Jaén, C. R., & Emrich, L. J. (1985). Reports of smoking withdrawal symptoms over a 21 day period of abstinence. *Addictive Behaviors*, *10*(4), 373–381. https://doi.org/10.1016/0306-4603(85)90034-6

Davis, J. A., & Gould, T. J. (2006). The effects of DHBE and MLA on nicotine-induced enhancement of contextual fear conditioning in C57BL/6 mice. *Psychopharmacology*, *184*(3–4), 345–352. https://doi.org/10.1007/s00213-005-0047-y

Davis, J. A., & Gould, T. J. (2007). B2 subunit-containing nicotinic receptors mediate the enhancing effect of nicotine on trace cued fear conditioning in C57BL/6 mice. *Psychopharmacology*, *190*(3), 343–352. https://doi.org/10.1007/s00213-006-0624-8

Davis, J. A., James, J. R., Siegel, S. J., & Gould, T. J. (2005). Withdrawal from Chronic Nicotine Administration Impairs Contextual Fear Conditioning in C57BL/6 Mice. *The Journal of Neuroscience*, *25*(38), 8708–8713. https://doi.org/10.1523/JNEUROSCI.2853-05.2005

Drasdo, A., Caulfield, M., Bertrand, D., Bertrand, S., & Wonnacott, S. (1992). Methyl lycaconitine: A novel nicotinic antagonist. *Molecular and Cellular Neurosciences*, *3*(3), 237–243. https://doi.org/10.1016/1044-7431(92)90043-2

Dobin, A., Davis, C. A., Schlesinger, F., Drenkow, J., Zaleski, C., Jha, S., ... & Gingeras, T. R. (2013). STAR: ultrafast universal RNA-seq aligner. *Bioinformatics*, *29*(1), 15-21.

Ezama, L., Hernández-Cabrera, J. A., Seoane, S., Pereda, E., & Janssen, N. (2021). Functional connectivity of the hippocampus and its subfields in resting-state networks. *The European journal of neuroscience*, *53*(10), 3378–3393. https://doi.org/10.1111/ejn.15213

Ferbinteanu, J., & McDonald, R. J. (2001). Dorsal/ventral hippocampus, fornix, and conditioned place preference. *Hippocampus*, *11*(2), 187–200. https://doi.org/10.1002/hipo.1036

Froeliger, B., McConnell, P. A., Stankeviciute, N., McClure, E. A., Kalivas, P. W., & Gray, K. M. (2015). The effects of N -Acetylcysteine on frontostriatal resting-state functional connectivity, withdrawal symptoms and smoking abstinence: A double-blind, placebo-controlled fMRI pilot study. *Drug and Alcohol Dependence*, *156*, 234–242. https://doi.org/10.1016/j.drugalcdep.2015.09.021

Fujii, S., Ji, Z., & Sumikawa, K. (2000). Inactivation of α7 ACh receptors and activation of non-α7 ACh receptors both contribute to long term potentiation induction in the hippocampal CA1 region. *Neuroscience Letters*, *286*(2), 134–138. https://doi.org/10.1016/S0304-3940(00)01076-4

Gahring, L. C., Persiyanov, K., Dunn, D., Weiss, R., Meyer, E. L., & Rogers, S. W. (2004). Mouse strain-specific nicotinic acetylcholine receptor expression by inhibitory interneurons and astrocytes in the dorsal hippocampus. *The Journal of Comparative Neurology*, *468*(3), 334–346. https://doi.org/10.1002/cne.10943

Gahring, L. C., Persiyanov, K., & Rogers, S. W. (2004). Neuronal and astrocyte expression of nicotinic receptor subunit beta4 in the adult mouse brain. *The Journal of Comparative Neurology*, *468*(3), 322–333. https://doi.org/10.1002/cne.10942

Gai, D., Haan, E., Scholar, M., Nicholl, J., & Yu, S. (2015). Phenotypes of *AKT3* deletion: A case report and literature review. *American Journal of Medical Genetics Part A*, *167*(1), 174–179. https://doi.org/10.1002/ajmg.a.36710

Grabus, S. D., Martin, B. R., Batman, A. M., Tyndale, R. F., Sellers, E., & Damaj, M. I. (2005). Nicotine physical dependence and tolerance in the mouse following chronic oral administration. *Psychopharmacology*, *178*(2–3), 183–192. https://doi.org/10.1007/s00213-004-2007-3

Grieder, T. E., Herman, M. A., Contet, C., Tan, L. A., Vargas-Perez, H., Cohen, A., Chwalek, M., Maal-Bared, G., Freiling, J., Schlosburg, J. E., Clarke, L., Crawford, E., Koebel, P., Repunte-Canonigo, V., P Sanna, P., Tapper, A. R., Roberto, M., Kieffer, B. L., Sawchenko, P. E., … George, O. (2014). VTA CRF neurons mediate the aversive effects of nicotine withdrawal and promote intake escalation. *Nature Neuroscience*, *17*(12), 1751–1758. https://doi.org/10.1038/nn.3872

Gusel'nikova, V. V., & Korzhevskiy, D. E. (2015). NeuN As a Neuronal Nuclear Antigen and Neuron Differentiation Marker. *Acta Naturae*, *7*(2), 42–47.

Halassa, M. M., Fellin, T., & Haydon, P. G. (2007). The tripartite synapse: Roles for gliotransmission in health and disease. *Trends in Molecular Medicine*, *13*(2), 54–63. https://doi.org/10.1016/j.molmed.2006.12.005

Hancock, D. B., Markunas, C. A., Bierut, L. J., & Johnson, E. O. (2018). Human Genetics of Addiction: New Insights and Future Directions. *Current Psychiatry Reports*, *20*(2), 8. https://doi.org/10.1007/s11920-018-0873-3

Hatsukami, D. K., Hughes, J. R., & Pickens, R. W. (1985). Blood nicotine, smoke exposure and tobacco withdrawal symptoms. *Addictive Behaviors*, *10*(4), 413–417. https://doi.org/10.1016/0306-4603(85)90038-3

Hatsukami, D. K., Hughes, J. R., Pickens, R. W., & Svikis, D. (1984). Tobacco withdrawal symptoms: An experimental analysis. *Psychopharmacology*, *84*(2), 231–236. https://doi.org/10.1007/BF00427451

Hatsukami, DorothyK., Dahlgren, L., Zimmerman, R., & Hughes, JohnR. (1988). Symptoms of tobacco withdrawal from total cigarette cessation versus partial cigarette reduction. *Psychopharmacology*, *94*(2). https://doi.org/10.1007/BF00176853

Hindocha, C., Freeman, T. P., Grabski, M., Crudgington, H., Davies, A. C., Stroud, J. B., Das, R. K., Lawn, W., Morgan, C. J. A., & Curran, H. V. (2018). The effects of cannabidiol on

impulsivity and memory during abstinence in cigarette dependent smokers. *Scientific Reports*, *8*(1), 7568. https://doi.org/10.1038/s41598-018-25846-2

Hitchcock, L. N., & Lattal, K. M. (2018). Involvement of the dorsal hippocampus in expression and extinction of cocaine-induced conditioned place preference. *Hippocampus*, *28*(3), 226–238. https://doi.org/10.1002/hipo.22826

Hoeffer, C. A., & Klann, E. (2010). mTOR signaling: At the crossroads of plasticity, memory and disease. *Trends in Neurosciences*, *33*(2), 67–75. https://doi.org/10.1016/j.tins.2009.11.003

Holliday, E. D., & Gould, T. J. (2017). Chronic Nicotine Treatment During Adolescence Attenuates the Effects of Acute Nicotine in Adult Contextual Fear Learning. *Nicotine & Tobacco Research: Official Journal of the Society for Research on Nicotine and Tobacco*, *19*(1), 87–93. https://doi.org/10.1093/ntr/ntw176

Iacobas, D. A., Iacobas, S., Stout, R. F., & Spray, D. C. (2020). Cellular Environment Remodels the Genomic Fabrics of Functional Pathways in Astrocytes. *Genes*, *11*(5), 520. https://doi.org/10.3390/genes11050520

Jamal, A., King, B. A., Neff, L. J., Whitmill, J., Babb, S. D., & Graffunder, C. M. (2016). Current Cigarette Smoking Among Adults—United States, 2005–2015. *MMWR. Morbidity and Mortality Weekly Report*, *65*(44), 1205–1211. https://doi.org/10.15585/mmwr.mm6544a2

Jeong, K. H., Cho, K., Lee, M., Kim, S. Y., & Kim, W. (2021). Vascular endothelial growth factor receptor-3 regulates astroglial glutamate transporter-1 expression via mTOR activation in reactive astrocytes following pilocarpine-induced status epilepticus. *Glia*, *69*(2), 296–309. https://doi.org/10.1002/glia.23897

Ji, R.-R., Donnelly, C. R., & Nedergaard, M. (2019). Astrocytes in chronic pain and itch. *Nature Reviews Neuroscience*, *20*(11), 667–685. https://doi.org/10.1038/s41583-019-0218-1

Jia, Y., Sun, H., Wu, H., Zhang, H., Zhang, X., Xiao, D., Ma, X., & Wang, Y. (2016). Nicotine Inhibits Cisplatin-Induced Apoptosis via Regulating α5-nAChR/AKT Signaling in Human Gastric Cancer Cells. *PLOS ONE*, *11*(2), e0149120. https://doi.org/10.1371/journal.pone.0149120

Kihara, T., Shimohama, S., Sawada, H., Honda, K., Nakamizo, T., Shibasaki, H., Kume, T., & Akaike, A. (2001). A7 Nicotinic Receptor Transduces Signals to Phosphatidylinositol 3-Kinase to Block A β-Amyloid-induced Neurotoxicity. *Journal of Biological Chemistry*, *276*(17), 13541–13546. https://doi.org/10.1074/jbc.M008035200

Kim, H., Huh, Y.-J., Kim, J. H., Jo, M., Shin, J.-H., Park, S. C., Ahn, J.-Y., Lee, Y.-I., & Lee, Y. (2022). Identification and evaluation of midbrain specific longevity-related genes in exceptionally long-lived but healthy mice. *Frontiers in Aging Neuroscience*, *14*, 1030807. https://doi.org/10.3389/fnagi.2022.1030807

Kume, T., & Takada-Takatori, Y. (2018). Nicotinic Acetylcholine Receptor Signaling: Roles in Neuroprotection. In A. Akaike, S. Shimohama, & Y. Misu (Eds.), *Nicotinic Acetylcholine Receptor Signaling in Neuroprotection* (pp. 59–71). Springer Singapore. https://doi.org/10.1007/978-981-10-8488-1_4

Kutlu, M. G., Holliday, E., & Gould, T. J. (2016). High-affinity α4β2 nicotinic receptors mediate the impairing effects of acute nicotine on contextual fear extinction. *Neurobiology of Learning and Memory*, *128*, 17–22. https://doi.org/10.1016/j.nlm.2015.11.021

Kutlu, M. G., Ortega, L. A., & Gould, T. J. (2015). Strain-dependent performance in nicotine-induced conditioned place preference. *Behavioral Neuroscience*, *129*(1), 37–41. https://doi.org/10.1037/bne0000029

Leach, P. T., Cordero, K. A., & Gould, T. J. (2013). The effects of acute nicotine, chronic nicotine, and withdrawal from chronic nicotine on performance of a cued appetitive response. *Behavioral Neuroscience*, *127*(2), 303–310. https://doi.org/10.1037/a0031913

Levenga, J., Wong, H., Milstead, R. A., Keller, B. N., LaPlante, L. E., & Hoeffer, C. A. (2017). AKT isoforms have distinct hippocampal expression and roles in synaptic plasticity. *eLife*, *6*, e30640. https://doi.org/10.7554/eLife.30640

Levenga, J., Wong, H., Milstead, R., LaPlante, L., & Hoeffer, C. A. (2021). Immunohistological Examination of AKT Isoforms in the Brain: Cell-Type Specificity That May Underlie AKT's Role in Complex Brain Disorders and Neurological Disease. *Cerebral Cortex Communications*, *2*(2), tgab036. https://doi.org/10.1093/texcom/tgab036

Levin, E. D., Lee, C., Rose, J. E., Reyes, A., Ellison, G., Jarvik, M., & Gritz, E. (1990). Chronic nicotine and withdrawal effects on radial-arm maze performance in rats. *Behavioral and Neural Biology*, *53*(2), 269–276. https://doi.org/10.1016/0163-1047(90)90509-5

Levin, E. D., Petro, A., Rezvani, A. H., Pollard, N., Christopher, N. C., Strauss, M., Avery, J., Nicholson, J., & Rose, J. E. (2009). Nicotinic α7- or β2-containing receptor knockout: Effects on radial-arm maze learning and long-term nicotine consumption in mice. *Behavioural Brain Research*, *196*(2), 207–213. https://doi.org/10.1016/j.bbr.2008.08.048

Li, C.-Y., Li, X., Liu, S.-F., Qu, W.-S., Wang, W., & Tian, D.-S. (2015). Inhibition of mTOR pathway restrains astrocyte proliferation, migration and production of inflammatory mediators after oxygen–glucose deprivation and reoxygenation. *Neurochemistry International*, *83–84*, 9–18. https://doi.org/10.1016/j.neuint.2015.03.001

Li, Y., Song, A. M., Fu, Y., Walayat, A., Yang, M., Jian, J., Liu, B., Xia, L., Zhang, L., & Xiao, D. (2019). Perinatal nicotine exposure alters Akt/GSK-3β/mTOR/autophagy signaling, leading to development of hypoxic-ischemic-sensitive phenotype in rat neonatal brain. *American Journal of Physiology-Regulatory, Integrative and Comparative Physiology*, *317*(6), R803–R813. https://doi.org/10.1152/ajpregu.00218.2019

Liao, Y., Smyth, G. K., & Shi, W. (2014). featureCounts: an efficient general purpose program for assigning sequence reads to genomic features. *Bioinformatics*, *30*(7), 923-930.

Lin, W.-C., Hsu, T.-W., Chen, C.-L., Wu, C. W., Lu, C.-H., Chen, H.-L., Li, S.-H., Yeh, P.-Y., Cheng, Y.-F., & Lin, C.-P. (2012). Connectivity of Default-Mode Network Is Associated with Cerebral Edema in Hepatic Encephalopathy. *PLoS ONE*, *7*(5), e36986. https://doi.org/10.1371/journal.pone.0036986

Liu, J., Tao, X., Liu, F., Hu, Y., Xue, S., Wang, Q., Li, B., & Zhang, R. (2019). Behavior and Hippocampal Epac Signaling to Nicotine CPP in Mice. *Translational Neuroscience*, *10*, 254–259. https://doi.org/10.1515/tnsci-2019-0041

Liu, Q., Liu, C., Jiang, L., Li, M., Long, T., He, W., Qin, G., Chen, L., & Zhou, J. (2018). α7 Nicotinic acetylcholine receptor-mediated anti-inflammatory effect in a chronic migraine rat model via the attenuation of glial cell activation. *Journal of Pain Research*, *Volume 11*, 1129–1140. https://doi.org/10.2147/JPR.S159146

Loram, L. C., Taylor, F. R., Strand, K. A., Maier, S. F., Speake, J. D., Jordan, K. G., James, J. W., Wene, S. P., Pritchard, R. C., Green, H., Van Dyke, K., Mazarov, A., Letchworth, S. R., & Watkins, L. R. (2012). Systemic Administration of an Alpha-7 Nicotinic Acetylcholine Agonist Reverses Neuropathic Pain in Male Sprague Dawley Rats. *The Journal of Pain*, *13*(12), 1162–1171. https://doi.org/10.1016/j.jpain.2012.08.009

Love, M. I., Huber, W., & Anders, S. (2014). Moderated estimation of fold change and dispersion for RNA-seq data with DESeq2. *Genome biology*, *15*, 1-21.

Mahmoud, S., Gharagozloo, M., Simard, C., & Gris, D. (2019). Astrocytes Maintain Glutamate Homeostasis in the CNS by Controlling the Balance between Glutamate Uptake and Release. *Cells*, *8*(2), 184. https://doi.org/10.3390/cells8020184

Malin, D. H., Lake, J. R., Carter, V. A., Cunningham, J. S., Hebert, K. M., Conrad, D. L., & Wilson, O. B. (1994). The nicotinic antagonist mecamylamine precipitates nicotine

abstinence syndrome in the rat. *Psychopharmacology*, *115*(1–2), 180–184. https://doi.org/10.1007/BF02244770

Markou, A. (2008). Neurobiology of nicotine dependence. *Philosophical Transactions of the Royal Society B: Biological Sciences*, *363*(1507), 3159–3168. https://doi.org/10.1098/rstb.2008.0095

Markou, A., & Paterson, N. E. (2001). The nicotinic antagonist methyllycaconitine has differential effects on nicotine self-administration and nicotine withdrawal in the rat. *Nicotine & Tobacco Research*, *3*(4), 361–373. https://doi.org/10.1080/14622200110073380

Marubio, L. M., Gardier, A. M., Durier, S., David, D., Klink, R., Arroyo-Jimenez, M. M., McIntosh, J. M., Rossi, F., Champtiaux, N., Zoli, M., & Changeux, J. (2003). Effects of nicotine in the dopaminergic system of mice lacking the alpha4 subunit of neuronal nicotinic acetylcholine receptors. *European Journal of Neuroscience*, *17*(7), 1329–1337. https://doi.org/10.1046/j.1460-9568.2003.02564.x

Mathews, H. L., & Stitzel, J. A. (2019). The effects of oral nicotine administration and abstinence on sleep in male C57BL/6J mice. *Psychopharmacology*, *236*(4), 1335–1347. https://doi.org/10.1007/s00213-018-5139-6

Matta, S. G., Balfour, D. J., Benowitz, N. L., Boyd, R. T., Buccafusco, J. J., Caggiula, A. R., Craig, C. R., Collins, A. C., Damaj, M. I., Donny, E. C., Gardiner, P. S., Grady, S. R., Heberlein, U., Leonard, S. S., Levin, E. D., Lukas, R. J., Markou, A., Marks, M. J., McCallum, S. E., … Zirger, J. M. (2007). Guidelines on nicotine dose selection for in vivo research. *Psychopharmacology*, *190*(3), 269–319. https://doi.org/10.1007/s00213-006-0441-0

Maurer, J., Hupp, S., Bischoff, C., Foertsch, C., Mitchell, T., Chakraborty, T., & Iliev, A. (2017). Distinct Neurotoxicity Profile of Listeriolysin O from Listeria monocytogenes. *Toxins*, *9*(1), 34. https://doi.org/10.3390/toxins9010034

Miller, K. A., Degan, S., Wang, Y., Cohen, J., Ku, S. Y., Goodrich, D. W., & Gelman, I. H. (2023). PTEN-regulated PI3K-p110 and AKT isoform plasticity controls metastatic prostate cancer progression. *Oncogene*. https://doi.org/10.1038/s41388-023-02875-4

Miura, M., Ishii, K., Aosaki, T., & Sumikawa, K. (2006). Chronic nicotine treatment increases GABAergic input to striatal neurons. *NeuroReport*, *17*(5), 537–540. https://doi.org/10.1097/01.wnr.0000204984.21748.e3

Nardone, N., Shahid, M., Strasser, A. A., Dempsey, D. A., & Benowitz, N. L. (2020). The influence of nicotine metabolic rate on working memory over 6 hours of abstinence from nicotine. *Pharmacology Biochemistry and Behavior*, *188*, 172836. https://doi.org/10.1016/j.pbb.2019.172836

Naskar, S., & Chattarji, S. (2019). Stress Elicits Contrasting Effects on the Structure and Number of Astrocytes in the Amygdala versus Hippocampus. *eNeuro*, *6*(1), ENEURO.0338-18.2019. https://doi.org/10.1523/ENEURO.0338-18.2019

Norden, D. M., Trojanowski, P. J., Villanueva, E., Navarro, E., & Godbout, J. P. (2016). Sequential activation of microglia and astrocyte cytokine expression precedes increased Iba-1 or GFAP immunoreactivity following systemic immune challenge. *Glia*, *64*(2), 300–316. https://doi.org/10.1002/glia.22930

Opanashuk, L. A., Pauly, J. R., & Hauser, K. F. (2001). Effect of nicotine on cerebellar granule neuron development. *The European Journal of Neuroscience*, *13*(1), 48–56.

Osborn, L. M., Kamphuis, W., Wadman, W. J., & Hol, E. M. (2016). Astrogliosis: An integral player in the pathogenesis of Alzheimer's disease. *Progress in Neurobiology*, *144*, 121–141. https://doi.org/10.1016/j.pneurobio.2016.01.001

Paterson, N. E., & Markou, A. (2004). Prolonged nicotine dependence associated with extended access to nicotine self-administration in rats. *Psychopharmacology*, *173*(1–2), 64–72. https://doi.org/10.1007/s00213-003-1692-7

Patterson, F., Jepson, C., Loughead, J., Perkins, K., Strasser, A. A., Siegel, S., Frey, J., Gur, R., & Lerman, C. (2010). Working memory deficits predict short-term smoking resumption following brief abstinence. *Drug and Alcohol Dependence*, *106*(1), 61–64. https://doi.org/10.1016/j.drugalcdep.2009.07.020

Patti, L., Raiteri, L., Grilli, M., Zappettini, S., Bonanno, G., & Marchi, M. (2007). Evidence that α7 nicotinic receptor modulates glutamate release from mouse neocortical gliosomes. *Neurochemistry International*, *51*(1), 1–7. https://doi.org/10.1016/j.neuint.2007.03.003

Pavlov, V. A., Wang, H., Czura, C. J., Friedman, S. G., & Tracey, K. J. (2003). The cholinergic anti-inflammatory pathway: A missing link in neuroimmunomodulation. *Molecular Medicine (Cambridge, Mass.)*, *9*(5–8), 125–134.

Pekny, M., & Nilsson, M. (2005). Astrocyte activation and reactive gliosis. *Glia*, *50*(4), 427–434. https://doi.org/10.1002/glia.20207

Pekny, M., & Pekna, M. (2014). Astrocyte Reactivity and Reactive Astrogliosis: Costs and Benefits. *Physiological Reviews*, *94*(4), 1077–1098. https://doi.org/10.1152/physrev.00041.2013

Perea, G., Navarrete, M., & Araque, A. (2009). Tripartite synapses: Astrocytes process and control synaptic information. *Trends in Neurosciences*, *32*(8), 421–431. https://doi.org/10.1016/j.tins.2009.05.001

Pereira, A., & Furlan, F. A. (2010). Astrocytes and human cognition: Modeling information integration and modulation of neuronal activity. *Progress in Neurobiology*, *92*(3), 405–420. https://doi.org/10.1016/j.pneurobio.2010.07.001

Periyasamy, P., Guo, M.-L., & Buch, S. (2016). Cocaine induces astrocytosis through ER stress-mediated activation of autophagy. *Autophagy*, *12*(8), 1310–1329. https://doi.org/10.1080/15548627.2016.1183844

Persico, A. M. (1992). Predictors of Smoking Cessation in a Sample of Italian Smokers. *International Journal of the Addictions*, *27*(6), 683–695. https://doi.org/10.3109/10826089209068760

Pick, C. G., & Yanai, J. (1983). Eight Arm Maze for Mice. *International Journal of Neuroscience*, *21*(1–2), 63–66. https://doi.org/10.3109/00207458308986121

Pietilä, K., & Ahtee, L. (2000). Chronic nicotine administration in the drinking water affects the striatal dopamine in mice. *Pharmacology, Biochemistry, and Behavior*, *66*(1), 95–103. https://doi.org/10.1016/s0091-3057(00)00235-5

Prado, E., Maes, M., Piccoli, L. G., Baracat, M., Barbosa, D. S., Franco, O., Dodd, S., Berk, M., & Vargas Nunes, S. O. (2015). *N* -acetylcysteine for therapy-resistant tobacco use disorder: A pilot study. *Redox Report*, *20*(5), 215–222. https://doi.org/10.1179/1351000215Y.0000000004

Revathikumar, P., Bergqvist, F., Gopalakrishnan, S., Korotkova, M., Jakobsson, P.-J., Lampa, J., & Le Maître, E. (2016). Immunomodulatory effects of nicotine on interleukin 1β activated human astrocytes and the role of cyclooxygenase 2 in the underlying mechanism. *Journal of Neuroinflammation*, *13*(1), 256. https://doi.org/10.1186/s12974-016-0725-1

Robertson, A. J., Coluccio, A., Jensen, S., Rydlizky, K., & Coffman, J. A. (2013). Sea urchin akt activity is Runx-dependent and required for post-cleavage stage cell division. *Biology Open*, *2*(5), 472–478. https://doi.org/10.1242/bio.20133913

Rukstalis, M., Jepson, C., Patterson, F., & Lerman, C. (2005). Increases in hyperactive–impulsive symptoms predict relapse among smokers in nicotine replacement therapy. *Journal of Substance Abuse Treatment*, *28*(4), 297–304. https://doi.org/10.1016/j.jsat.2005.02.002

Santello, M., Toni, N., & Volterra, A. (2019). Astrocyte function from information processing to cognition and cognitive impairment. *Nature Neuroscience*, *22*(2), 154–166. https://doi.org/10.1038/s41593-018-0325-8

Schildge, S., Bohrer, C., Beck, K., & Schachtrup, C. (2013). Isolation and Culture of Mouse Cortical Astrocytes. *Journal of Visualized Experiments*, *71*, 50079. https://doi.org/10.3791/50079

Schummers, J., Yu, H., & Sur, M. (2008). Tuned Responses of Astrocytes and Their Influence on Hemodynamic Signals in the Visual Cortex. *Science*, *320*(5883), 1638–1643. https://doi.org/10.1126/science.1156120

Sharma, G., & Vijayaraghavan, S. (2001). Nicotinic cholinergic signaling in hippocampal astrocytes involves calcium-induced calcium release from intracellular stores. *Proceedings of the National Academy of Sciences of the United States of America*, *98*(7), 4148–4153. https://doi.org/10.1073/pnas.071540198

Shaw, S., Bencherif, M., & Marrero, M. B. (2002). Janus Kinase 2, an Early Target of α7 Nicotinic Acetylcholine Receptor-mediated Neuroprotection against Aβ-(1–42) Amyloid. *Journal of Biological Chemistry*, *277*(47), 44920–44924. https://doi.org/10.1074/jbc.M204610200

Shen, Q., Zhu, H., Lei, Q., Chen, L., Yang, D., & Sui, W. (2020). MicroRNA149 3p inhibits cell proliferation by targeting AKT2 in oral squamous cell carcinoma. *Molecular Medicine Reports*, *23*(3), 172. https://doi.org/10.3892/mmr.2020.11811

Shi, X., Ding, J., Zheng, Y., Wang, J., Sobhani, N., Neeli, P., Wang, G., Zheng, J., & Chai, D. (2023). HMGB1/GPC3 dual targeting vaccine induces dendritic cells-mediated CD8+T cell immune response and elicits potential therapeutic effect in hepatocellular carcinoma. *iScience*, *26*(3), 106143. https://doi.org/10.1016/j.isci.2023.106143

Shigetomi, E., Bowser, D. N., Sofroniew, M. V., & Khakh, B. S. (2008). Two Forms of Astrocyte Calcium Excitability Have Distinct Effects on NMDA Receptor-Mediated Slow Inward

Currents in Pyramidal Neurons. *Journal of Neuroscience*, *28*(26), 6659–6663. https://doi.org/10.1523/JNEUROSCI.1717-08.2008

Simard, M., & Nedergaard, M. (2004). The neurobiology of glia in the context of water and ion homeostasis. *Neuroscience*, *129*(4), 877–896. https://doi.org/10.1016/j.neuroscience.2004.09.053

Sofroniew, M. V. (2009). Molecular dissection of reactive astrogliosis and glial scar formation. *Trends in Neurosciences*, *32*(12), 638–647. https://doi.org/10.1016/j.tins.2009.08.002

Sofroniew, M. V. (2015). Astrogliosis. *Cold Spring Harbor Perspectives in Biology*, *7*(2), a020420. https://doi.org/10.1101/cshperspect.a020420

Sweet, L. H., Mulligan, R. C., Finnerty, C. E., Jerskey, B. A., David, S. P., Cohen, R. A., & Niaura, R. S. (2010). Effects of nicotine withdrawal on verbal working memory and associated brain response. *Psychiatry Research: Neuroimaging*, *183*(1), 69–74. https://doi.org/10.1016/j.pscychresns.2010.04.014

Tamim, S., Vo, D. T., Uren, P. J., Qiao, M., Bindewald, E., Kasprzak, W. K., Shapiro, B. A., Nakaya, H. I., Burns, S. C., Araujo, P. R., Nakano, I., Radek, A. J., Kuersten, S., Smith, A. D., & Penalva, L. O. F. (2014). Genomic analyses reveal broad impact of miR-137 on genes associated with malignant transformation and neuronal differentiation in glioblastoma cells. *PloS One*, *9*(1), e85591. https://doi.org/10.1371/journal.pone.0085591

Tarassishin, L., Suh, H.-S., & Lee, S. C. (2014). LPS and IL-1 differentially activate mouse and human astrocytes: Role of CD14: Species-Dependent Astrocyte Immune Activation. *Glia*, *62*(6), 999–1013. https://doi.org/10.1002/glia.22657

Tsurutani, J., Castillo, S. S., Brognard, J., Granville, C. A., Zhang, C., Gills, J. J., Sayyah, J., & Dennis, P. A. (2005). Tobacco components stimulate Akt-dependent proliferation and NFkappaB-dependent survival in lung cancer cells. *Carcinogenesis*, *26*(7), 1182–1195. https://doi.org/10.1093/carcin/bgi072

Verkhratsky, A., Ho, M. S., Vardjan, N., Zorec, R., & Parpura, V. (2019). General Pathophysiology of Astroglia. In A. Verkhratsky, M. S. Ho, R. Zorec, & V. Parpura (Eds.), *Neuroglia in Neurodegenerative Diseases* (Vol. 1175, pp. 149–179). Springer Singapore. https://doi.org/10.1007/978-981-13-9913-8_7

Verkhratsky, A., Rodrigues, J. J., Pivoriunas, A., Zorec, R., & Semyanov, A. (2019). Astroglial atrophy in Alzheimer's disease. *Pflugers Archiv: European Journal of Physiology*, *471*(10), 1247–1261. https://doi.org/10.1007/s00424-019-02310-2

Verkhratsky, A., Steardo, L., Parpura, V., & Montana, V. (2016). Translational potential of astrocytes in brain disorders. *Progress in Neurobiology*, *144*, 188–205. https://doi.org/10.1016/j.pneurobio.2015.09.003

Welsby, P., Rowan, M., & Anwyl, R. (2006). Nicotinic receptor-mediated enhancement of long-term potentiation involves activation of metabotropic glutamate receptors and ryanodine-sensitive calcium stores in the dentate gyrus. *European Journal of Neuroscience*, *24*(11), 3109–3118. https://doi.org/10.1111/j.1460-9568.2006.05187.x

West, K. A., Brognard, J., Clark, A. S., Linnoila, I. R., Yang, X., Swain, S. M., Harris, C., Belinsky, S., & Dennis, P. A. (2003). Rapid Akt activation by nicotine and a tobacco carcinogen modulates the phenotype of normal human airway epithelial cells. *The Journal of Clinical Investigation*, *111*(1), 81–90. https://doi.org/10.1172/JCI16147

Wincott, C. M., Abera, S., Vunck, S. A., Tirko, N., Choi, Y., Titcombe, R. F., Antoine, S. O., Tukey, D. S., DeVito, L. M., Hofmann, F., Hoeffer, C. A., & Ziff, E. B. (2014). cGMP-dependent protein kinase type II knockout mice exhibit working memory impairments, decreased repetitive behavior, and increased anxiety-like traits. *Neurobiology of Learning and Memory*, *114*, 32–39. https://doi.org/10.1016/j.nlm.2014.04.007

Wong, H., Levenga, J., LaPlante, L., Keller, B., Cooper-Sansone, A., Borski, C., Milstead, R., Ehringer, M., & Hoeffer, C. (2020). Isoform-specific roles for AKT in affective behavior,

spatial memory, and extinction related to psychiatric disorders. *eLife*, *9*, e56630. https://doi.org/10.7554/eLife.56630

Xu, S., Ni, H., Chen, H., & Dai, Q. (2019). The interaction between STAT3 and nAChRα1 interferes with nicotine-induced atherosclerosis via Akt/mTOR signaling cascade. *Aging*, *11*(19), 8120–8138. https://doi.org/10.18632/aging.102296

Young, J. W., Finlayson, K., Spratt, C., Marston, H. M., Crawford, N., Kelly, J. S., & Sharkey, J. (2004). Nicotine Improves Sustained Attention in Mice: Evidence for Involvement of the α7 Nicotinic Acetylcholine Receptor. *Neuropsychopharmacology*, *29*(5), 891–900. https://doi.org/10.1038/sj.npp.1300393

Zeisel, A., Muñoz-Manchado, A. B., Codeluppi, S., Lönnerberg, P., La Manno, G., Juréus, A., Marques, S., Munguba, H., He, L., Betsholtz, C., Rolny, C., Castelo-Branco, G., Hjerling-Leffler, J., & Linnarsson, S. (2015). Brain structure. Cell types in the mouse cortex and hippocampus revealed by single-cell RNA-seq. *Science (New York, N.Y.)*, *347*(6226), 1138–1142. https://doi.org/10.1126/science.aaa1934

Zhang, D., Wang, J., Zhou, C., & Xiao, W. (2017). Zebrafish akt2 is essential for survival, growth, bone development, and glucose homeostasis. *Mechanisms of Development*, *143*, 42–52. https://doi.org/10.1016/j.mod.2017.01.004

Zhang, J., Han, L., Zhang, A., Wang, Y., Yue, X., You, Y., Pu, P., & Kang, C. (2010). AKT2 expression is associated with glioma malignant progression and required for cell survival and invasion. *Oncology Reports*, *24*(1), 65–72. https://doi.org/10.3892/or_00000829

Zhang, K., Förster, R., He, W., Liao, X., Li, J., Yang, C., Qin, H., Wang, M., Ding, R., Li, R., Jian, T., Wang, Y., Zhang, J., Yang, Z., Jin, W., Zhang, Y., Qin, S., Lu, Y., Chen, T., … Chen, X. (2021). Fear learning induces α7-nicotinic acetylcholine receptor-mediated astrocytic responsiveness that is required for memory persistence. *Nature Neuroscience*, *24*(12), 1686–1698. https://doi.org/10.1038/s41593-021-00949-8

Zhou, X., Nonnemaker, J., Sherrill, B., Gilsenan, A. W., Coste, F., & West, R. (2009). Attempts to quit smoking and relapse: Factors associated with success or failure from the ATTEMPT cohort study. *Addictive Behaviors*, *34*(4), 365–373. https://doi.org/10.1016/j.addbeh.2008.11.013

Zhu, H., Zhuang, D., Lou, Z., Lai, M., Fu, D., Hong, Q., Liu, H., & Zhou, W. (2021). Akt and its phosphorylation in nucleus accumbens mediate heroin-seeking behavior induced by cues in rats. *Addiction Biology*, *26*(5), e13013. https://doi.org/10.1111/adb.13013

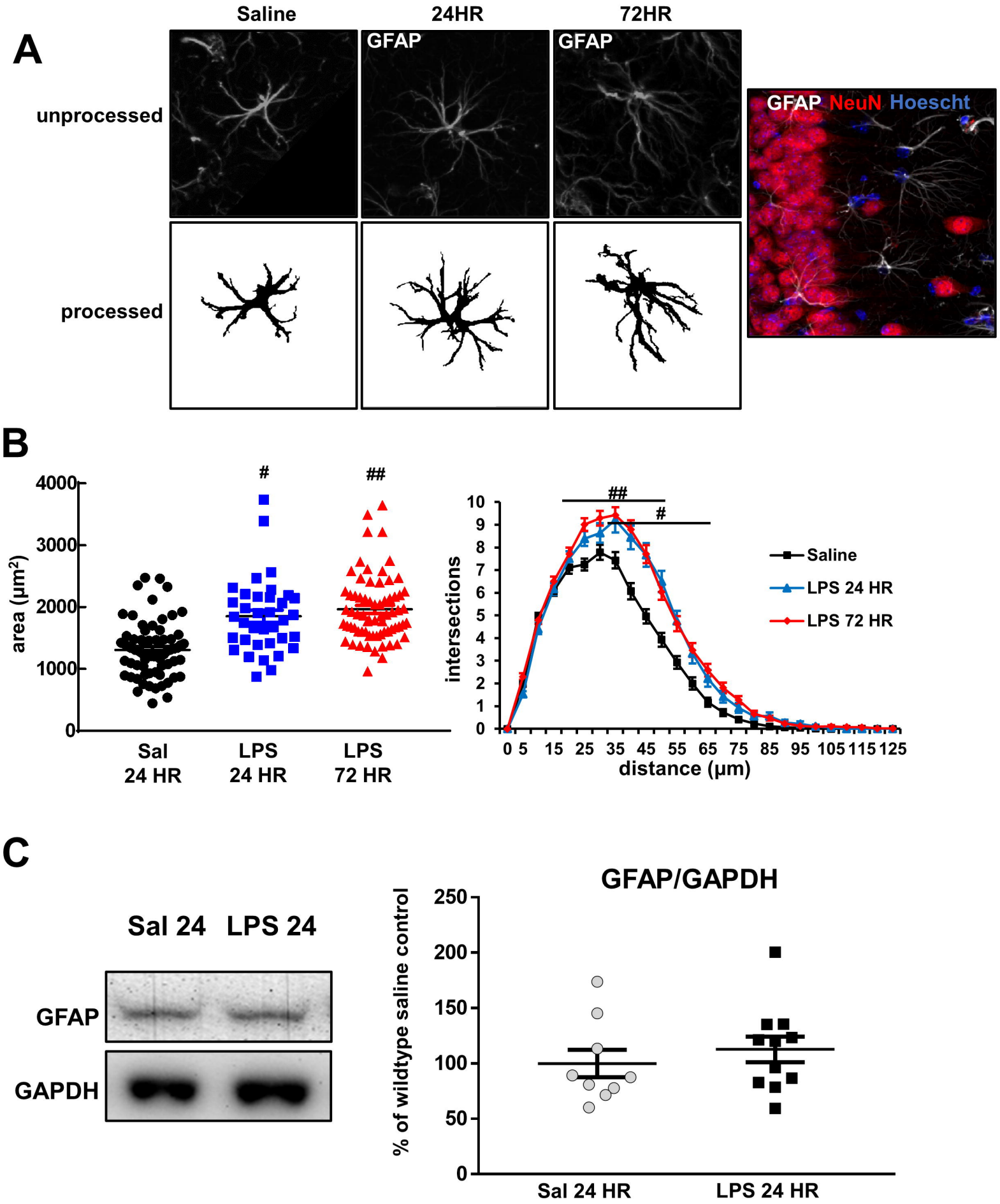
A
Saline
24HR
72HR
GFAP
GFAP
unprocessed
processed
GFAP NeuN Hoescht
B
area (μm²)
4000
3000
2000
1000
0
#
##
Sal 24 HR
LPS 24 HR
LPS 72 HR
intersections
10
9
8
7
6
5
4
3
2
1
0
##
#
Saline
LPS 24 HR
LPS 72 HR
0 5 15 25 35 45 55 65 75 85 95 105 115 125
distance (μm)
C
Sal 24 LPS 24
GFAP
GAPDH
GFAP/GAPDH
% of wildtype saline control
250
200
150
100
50
0
Sal 24 HR
LPS 24 HR

Figure 1

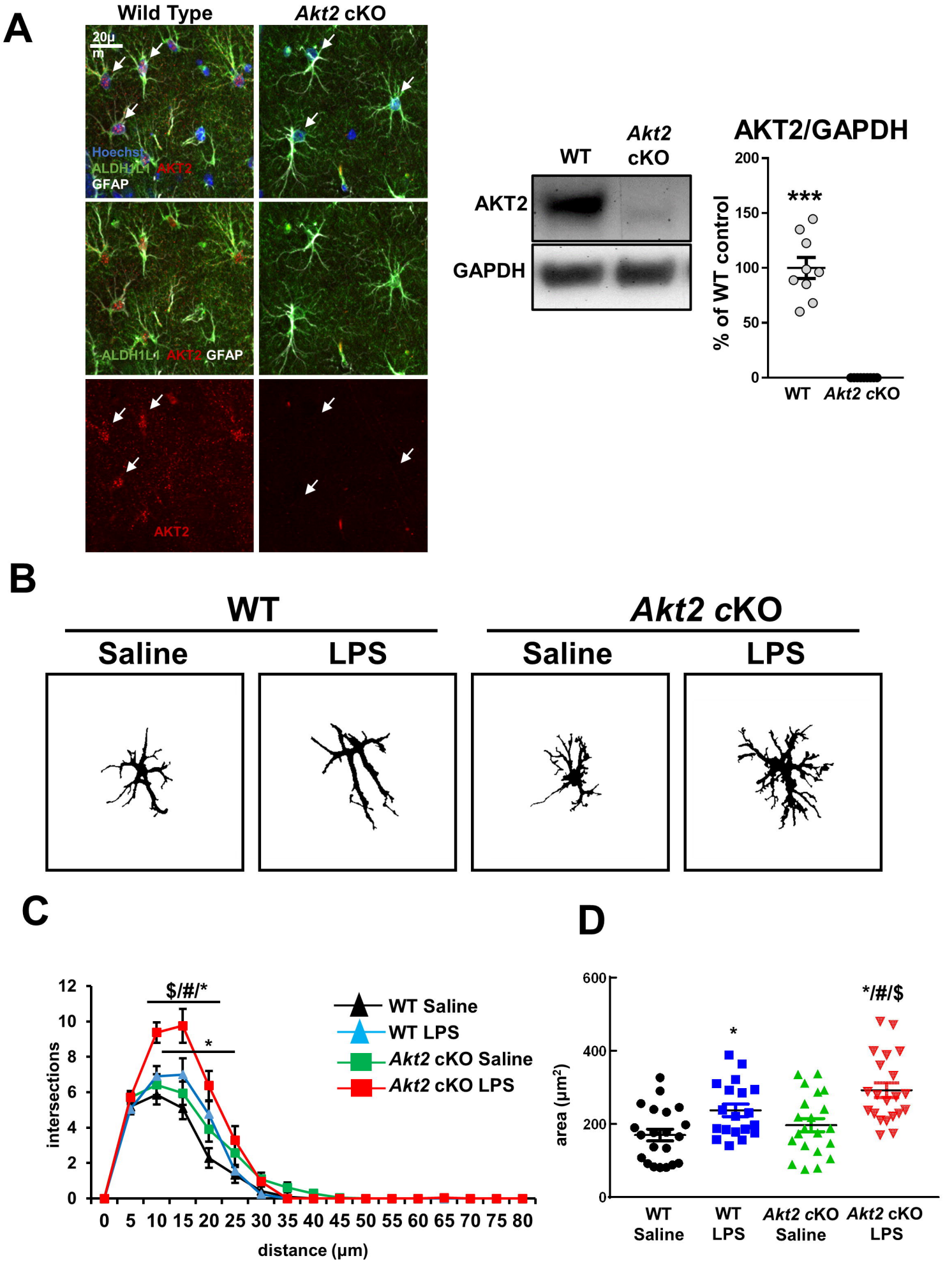
A
Wild Type
Akt2 cKO
20μm
Hoechst
ALDH1L1 AKT2
GFAP
ALDH1L1 AKT2 GFAP
AKT2
WT
Akt2 cKO
AKT2
GAPDH
AKT2/GAPDH
% of WT control
***
WT
Akt2 cKO
B
WT
Akt2 cKO
Saline
LPS
Saline
LPS
C
$/#/*
*
WT Saline
WT LPS
Akt2 cKO Saline
Akt2 cKO LPS
intersections
distance (μm)
D
*/#/$
*
area (μm²)
WT Saline
WT LPS
Akt2 cKO Saline
Akt2 cKO LPS

Figure 2

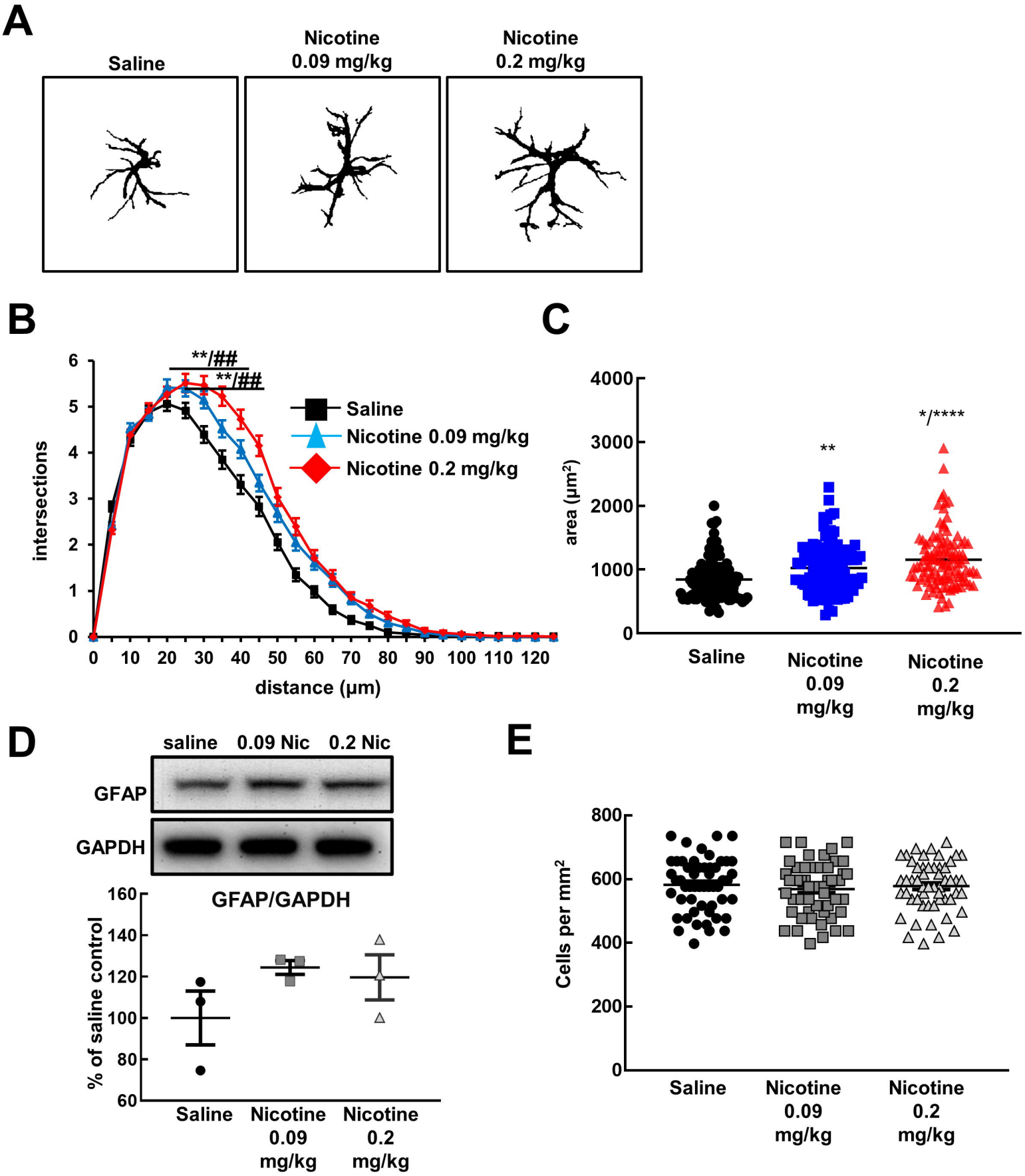
A
Saline
Nicotine 0.09 mg/kg
Nicotine 0.2 mg/kg
B
**/##
**/##
Saline
Nicotine 0.09 mg/kg
Nicotine 0.2 mg/kg
intersections
distance (µm)
C
area (µm²)
**
*/****
Saline
Nicotine 0.09 mg/kg
Nicotine 0.2 mg/kg
D
saline
0.09 Nic
0.2 Nic
GFAP
GAPDH
GFAP/GAPDH
% of saline control
Saline
Nicotine 0.09 mg/kg
Nicotine 0.2 mg/kg
E
Cells per mm²
Saline
Nicotine 0.09 mg/kg
Nicotine 0.2 mg/kg

Figure 3

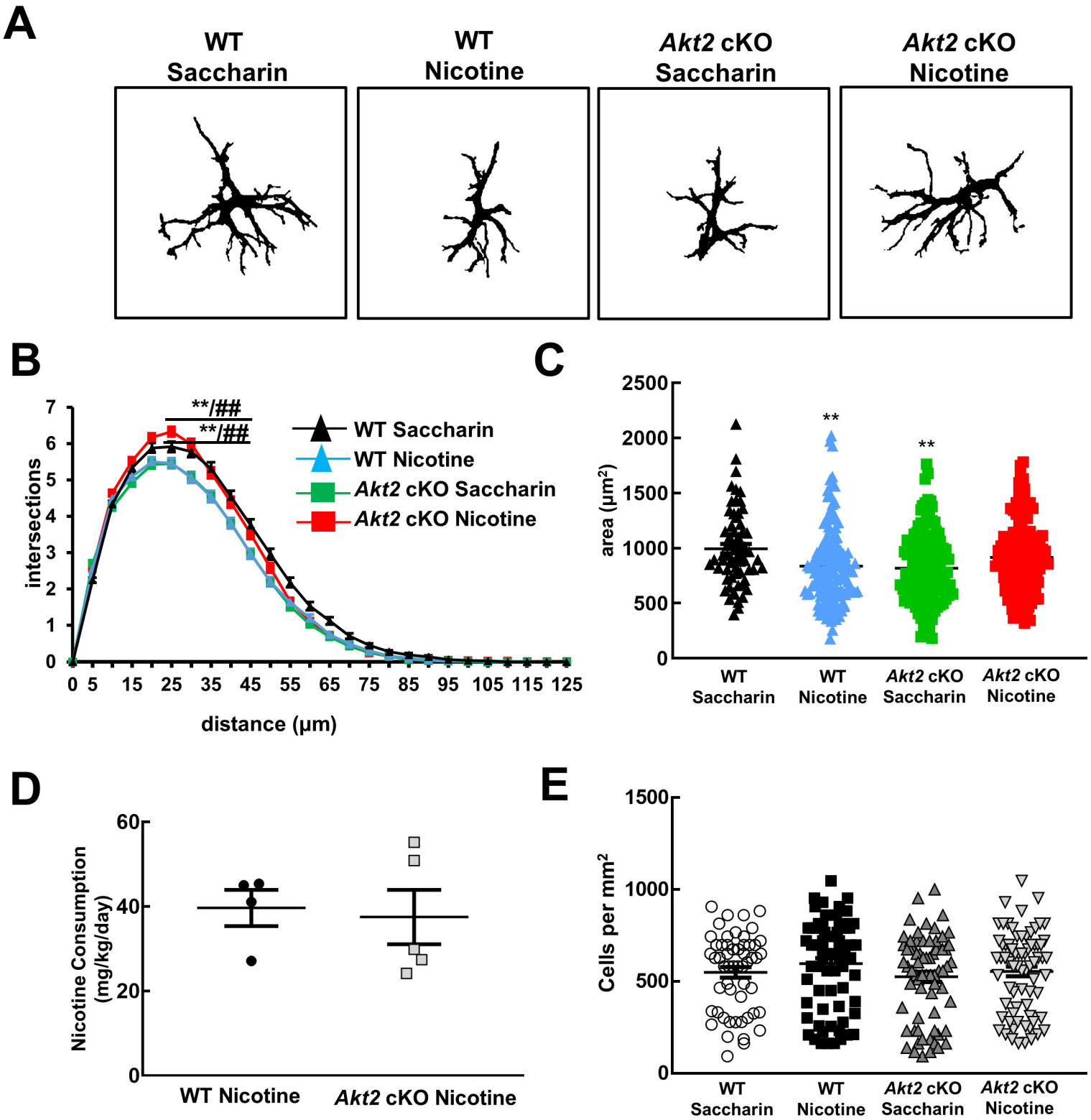
A
WT Saccharin
WT Nicotine
Akt2 cKO Saccharin
Akt2 cKO Nicotine
B
intersections
distance (μm)
**/##
**/##
WT Saccharin
WT Nicotine
Akt2 cKO Saccharin
Akt2 cKO Nicotine
C
area (μm²)
**
**
WT Saccharin
WT Nicotine
Akt2 cKO Saccharin
Akt2 cKO Nicotine
D
Nicotine Consumption (mg/kg/day)
WT Nicotine
Akt2 cKO Nicotine
E
Cells per mm²
WT Saccharin
WT Nicotine
Akt2 cKO Saccharin
Akt2 cKO Nicotine

Figure 4

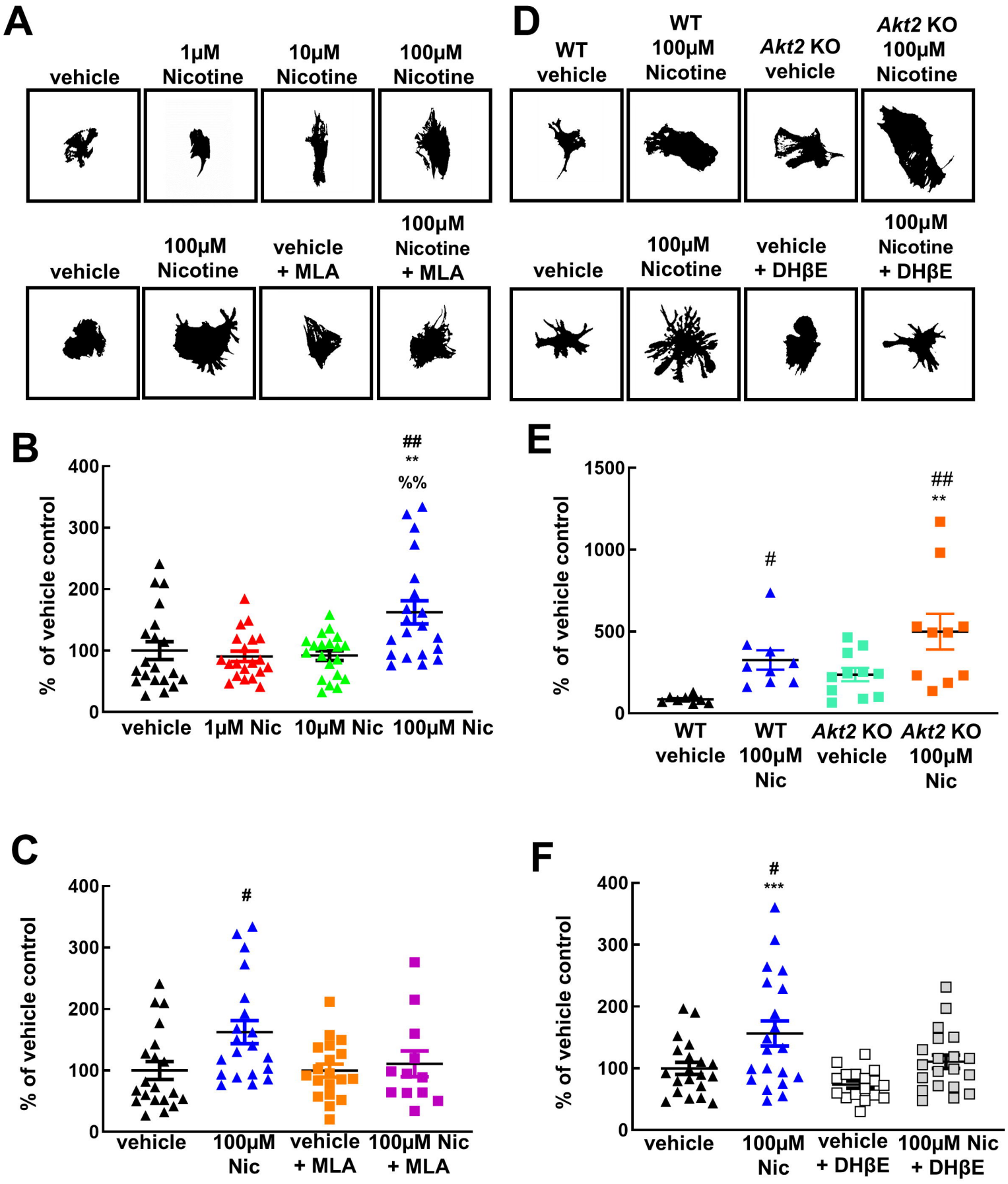
A
vehicle
1μM Nicotine
10μM Nicotine
100μM Nicotine
vehicle
100μM Nicotine
vehicle + MLA
100μM Nicotine + MLA
D
WT vehicle
WT 100μM Nicotine
Akt2 KO vehicle
Akt2 KO 100μM Nicotine
vehicle
100μM Nicotine
vehicle + DHβE
100μM Nicotine + DHβE
B
% of vehicle control
400
300
200
100
0
##
**
%%
vehicle
1μM Nic
10μM Nic
100μM Nic
E
% of vehicle control
1500
1000
500
0
#
##
**
WT vehicle
WT 100μM Nic
Akt2 KO vehicle
Akt2 KO 100μM Nic
C
% of vehicle control
400
300
200
100
0
#
vehicle
100μM Nic
vehicle + MLA
100μM Nic + MLA
F
% of vehicle control
400
300
200
100
0
#
***
vehicle
100μM Nic
vehicle + DHβE
100μM Nic + DHβE

Figure 5

A

Test Phase	Pre	Conditioning	Test1	Conditioning	Test2
Nicotine Group	No Inj	Nicotine/Saline	No Inj	Nicotine/Saline	No Inj
Saline Group	No Inj	Saline/Saline	No Inj	Saline/Saline	No Inj

Day 0 1 2 3 4 5 6 7 8 9

B

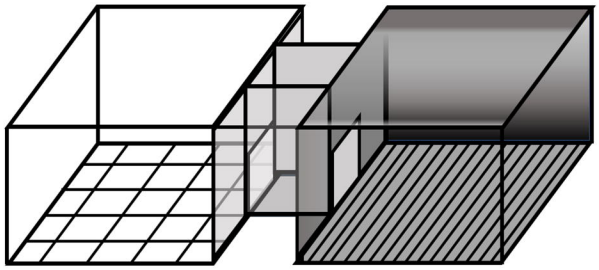

C

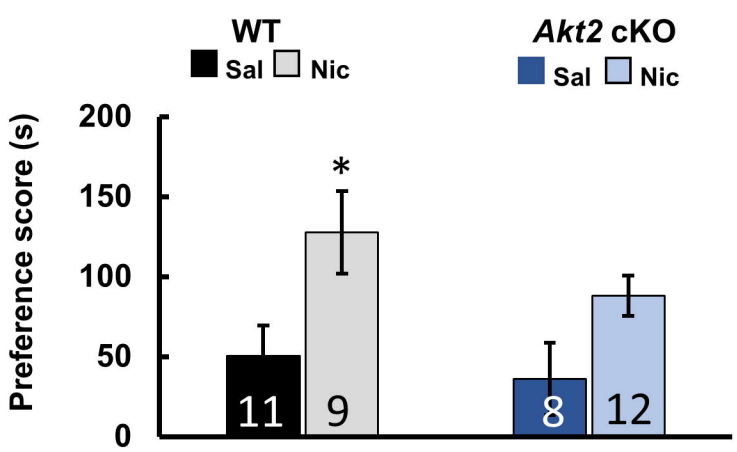

D

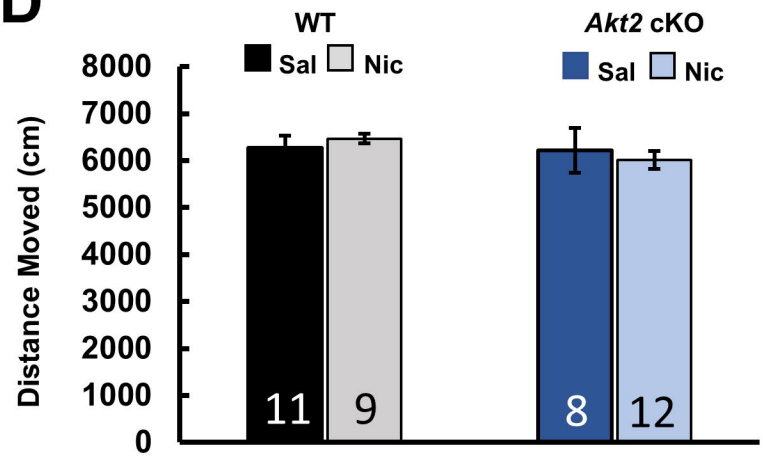

E

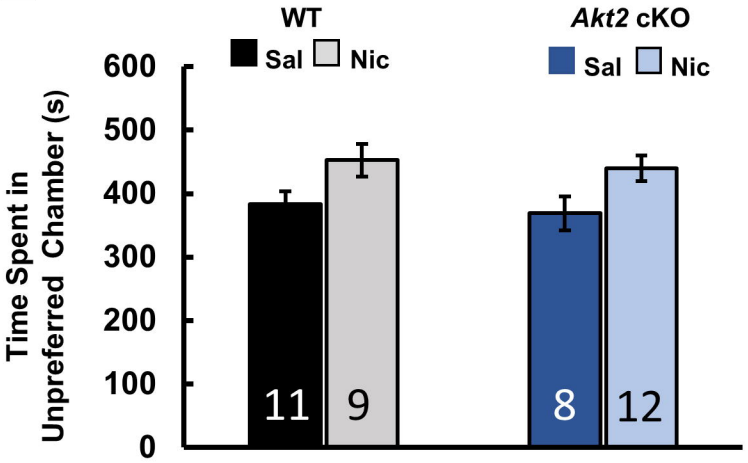

Figure 6